Uptake of niobium by cement systems relevant for nuclear waste disposal: Impact of ISA and chloride

Neşe Çevirim-Papaioannou [a,*], Yongheum Jo [a], Karsten Franke [b], Markus Fuss [a], Benny de Blochouse [c], Marcus Altmaier [a], Xavier Gaona [a,*]

[a] Institute for Nuclear Waste Disposal (INE), Karlsruhe Institute of Technology (KIT), Karlsruhe, Germany
[b] Institute of Resource Ecology, Helmholtz-Zentrum Dresden-Rossendorf (HZDR), Leipzig, Germany
[c] ONDRAF/NIRAS, Sint-Joost-ten-Node, Belgium

Keywords:
Niobium
Cement
ISA
Chloride
Sorption
Isotopic exchange

A B S T R A C T

The isotope ^{94}Nb ($t_{1/2}$ = 2.04 • 10^4 a) is produced during the operation of nuclear reactors due to the neutron activation of ^{93}Nb present in reactor vessels. Related waste streams will be disposed of in cement-based repositories for low and intermediate level wastes (L/ILW).

The retention of niobium by cement was investigated using a combination of ^{95}Nb and natural ^{93}Nb. Sorption experiments assessed also the impact of iso-saccharinic acid (ISA) and chloride on Nb retention, both expected in specific L/ILW.

Sorption experiments revealed a strong uptake of Nb by cement. Isotopic exchange with ^{93}Nb in HCP partly explains ^{95}Nb uptake, although sorption on C-S-H is tentatively proposed as main retention process. Sorption of Nb is weakly affected by chloride, but decreases importantly at [ISA] $\geq 10^{-3}$ M reflecting the formation of (Ca-)Nb(V)-ISA complexes. This work provides key inputs to assess ^{94}Nb retention in the Safety Case context of nuclear waste repositories.

1. Introduction

The naturally occurring, stable isotope of niobium, ^{93}Nb, is expected in some structural components present in nuclear reactor vessels, especially those constructed with Inconel alloys or with stainless steel containing niobium [1–3]. The isotope ^{94}Nb ($t_{1/2}$ 2.04 • 10^4 a) [4,5] is produced during the operation of nuclear reactors due to the (n,γ) neutron activation of ^{93}Nb, *i.e.* $^{93}Nb + n \rightarrow {}^{94}Nb + \gamma$-ray. The probability of a neutron being absorbed by ^{93}Nb is very low. But in view of the long half-life of ^{94}Nb, the inventory of ^{94}Nb increases linearly with reactor operation and thus a significant amount of this radionuclide can be accumulated by the time the reactor is decommissioned [3]. Accordingly, ^{94}Nb is expected in low and intermediate level wastes (L/ILW) resulting from the dismantling of nuclear reactors as well as in waste streams originating from the treatment of the primary cooling circuit [2,3,6]. Because of its decay properties (β^- emission to stable ^{94}Mo, with average and maximum kinetic energies of 156.0 and 500.0 keV, respectively), ^{94}Nb is classified in the group of *high radiotoxicity* radionuclides, together with ^{60}Co or ^{90}Sr [3]. In the context of a near-surface disposal facility, ^{94}Nb was identified as relevant contributor (together with ^{239}Pu and ^{240}Pu) to the effective dose potentially released to the biosphere [7].

Cementitious materials are widely used in repositories for nuclear waste with several applications, *e.g.* conditioning the waste, as backfill material or for construction purposes. In contact with groundwater, cementitious materials are known to degrade following three main stages [8–11]. The first degradation stage is defined by the dissolution of alkali (Na, K) oxides/hydroxides, which set high pH values (13–13.5) and alkali concentrations ([Na + K] ≈ 0.3–0.5 M). After the complete dissolution of the alkali phases, the second degradation stage is controlled by the dissolution of portlandite, $Ca(OH)_2$, which buffers the pore water composition at pH ≈ 12.5 and [Ca] ≈ 0.02 M. The third degradation stage is dominated by the dissolution of the calcium silicate hydrate (C-S-H) phases, of which the ratio Ca:Si varies from ≈1.6 (pH ≈ 12.5 and [Ca] ≈ 0.02 M) to ≈0.6 (with pH ≈ 10 and [Ca] ≈ 10^{-4} M) [12,13].

Hydrolysis and formation of solubility-limiting solid phases are key processes governing the chemistry of metal ions in aqueous systems.

* Corresponding authors.
E-mail addresses: nese.cevirim@kit.edu (N. Çevirim-Papaioannou), xavier.gaona@kit.edu (X. Gaona).

Situated in the group 5 of the periodic table and with an electronic configuration of [Kr] $4d^4$ $5s^1$, niobium is exclusively found in the oxidation state +V in aqueous systems [14–16]. Niobium(V) is characterized by strong hydrolysis and the formation of sparingly soluble oxides, *e.g.* Nb_2O_5(s) [14,15]. The predominance of negatively charged hydrolysis species above pH ≈ 5 ($Nb(OH)_6^-$ and $Nb(OH)_7^{2-}$) significantly increases the solubility of Nb_2O_5(s) in the alkaline to hyperalkaline pH of relevance for cementitious systems [17]. At these pH conditions and under the absence of divalent cations, the predominance of polyniobiate aqueous species at [Nb(V)] > 1 mM (*e.g.* $Nb_6O_{19}^{8-}$, $Nb_6O_{19}OH^{9-}$) and the formation of highly soluble Na-polyniobiate solid phases (*e.g.* $Na_8Nb_6O_{19}{\cdot}13H_2O$(s), $Na_7HNb_6O_{19}{\cdot}15H_2O$(s)) have been reported in the literature [17,18]. The presence of Ca in alkaline systems triggers the precipitation of sparingly soluble Ca-Nb(V) solid phases, although the exact stoichiometry of these solid phases remains ill-defined. Lothenbach and co-workers conducted oversaturation solubility experiments with $[NbCl_5]_0$ 1.2 • 10^{-3} M in 0.02 M NaOH [19]. Niobium remained completely dissolved until the addition of 0.03 M $Ca(ClO_4)_2{\cdot}4H_2O$, which led to the immediate precipitation of a white solid identified by XRD as a poorly crystalline $CaNb_2O_6{\cdot}nH_2O$(s). The dissolved Nb concentration in equilibrium with this solid phase remained below the detection limit (≈5.4 • 10^{-8} M). Pointeau et al. studied the solubility of Nb(V) in pore water solutions of different cementitious systems (CEM I, CEM V and C-S-H, all with Ca:Si 0.7–1.3) [20]. Experiments were performed at $[Nb]_0$ 6.5 • 10^{-8} M, with pH (9.9–12.5) and [Ca] (7.7 • 10^{-5}–0.014 M). In all cases, very low Nb concentrations were measured (≈1 • 10^{-9}–1 • 10^{-8} M) after attaining equilibrium conditions. These concentrations are much lower than those expected to be controlled by Nb_2O_5(s), and the authors suggested a solubility control by a Ca–Nb(V) solid phase, although no solid phase characterization was performed. Talerico and co-workers studied the solubility of Nb(V) in alkaline solutions representative of cementitious systems, with 9.5 ≤ pH ≤ 13.2 and 1.5·10^{-4} M ≤ $[Ca]_{tot}$ ≤ 0.015 M [21]. All experiments were approached from oversaturation conditions with $[Nb]_0$ 5 • 10^{-4}–3 • 10^{-6} M. The authors observed a clear decrease in the niobium concentrations, which varied between 3·10^{-9}–2 • 10^{-5} M after attaining equilibrium conditions. The decrease in Nb concentration was attributed to the precipitation of a poorly crystalline Ca–Nb(V) solid phase tentatively identified as $CaNb_4O_{11}{\cdot}8H_2O$(s).

Sorption is a key process affecting the retention/mobilization of radionuclides in a repository for nuclear waste. A limited number of experimental studies have previously tackled the uptake of Nb(V) by cementitious materials. Pilkington and Stone conducted sorption experiments with niobium and a concrete formulation 10:1 PFA/OPC (Pulverised Fuel Ash/Ordinary Portland Cement) [22]. The pore water of this concrete formulation is characterized by slightly decreased pH (11.8) and clearly lower calcium concentrations (9.2 • 10^{-4} M), compared to standard cement formulations in the degradation stages I or II. Experiments were performed with stable ^{93}Nb(V) using a very high initial niobium concentration, 5.3 • 10^{-3} M. After a contact time of 2 months, the authors reported largely dispersed R_d values ranging from 500 to 80,000 L·kg^{-1}. Although there is a slight tendency to decreasing R_d values with increasing solid-to-liquid (S:L) ratio, there is no clear explanation (besides possible heterogeneities in the concrete samples) for the large dispersion reported. Baker et al. investigated the uptake of Nb(V) by NRVB, a cement-based backfill material considered in a conceptual UK geological disposal facility for nuclear waste [23]. Experiments were performed with saline water (0.5 M NaCl) to simulate groundwater conditions at Sellafield. The short-lived isotope ^{95}Nb ($t_{1/2}$ 35.15 days) was used in the sorption experiments, with $[Nb]_0$ 4.5 • 10^{-13} M. The authors reported very similar R_d values for the two phase-separation methods used, 0.45 μm (R_d 3.5 • 10^4 L·kg^{-1}) and 30,000 MWCO filtration (R_d 4.1 • 10^4 L·kg^{-1}). Pointeau and co-workers conducted the most comprehensive sorption study with Nb(V) and cementitious materials available to date [20]. The authors used two different cements (CEM I and CEM V) in three different degradation stages, as well as C-S-H phases with Ca:Si ratios of 0.7, 1.0 and 1.3. Experiments were performed using the short-lived isotope ^{95}Nb. Pointeau and co-workers did not report the initial niobium concentration, but stated that it was *above the solubility limit*. The concentrations of Nb measured after the uptake process were clearly below the solubility limit, and the authors reported R_d values ranging from 1 to 2.4 • 10^5 L·kg^{-1} (Ca:Si 1.3 and 1.0) and 4–7 • 10^4 L·kg^{-1} (Ca:Si 0.7). Desorption experiments resulted in very similar R_d values, thus confirming that equilibrium conditions were attained.

Two recent review works by Wieland [24] and Ochs, Mallants and Wang [9] have reported selected best estimates for the uptake of Nb(V) by cement in degradation stages I, II and III. In the "*Sorption Data Base for the Cementitious Near Field of L/ILW and ILW Repositories*", Wieland retained the same R_d values as previously selected in [8], *i.e.* 1000 L·kg^{-1} for the three degradation stages of cement. Although acknowledging that the new data by Pointeau, Landesman, Coreau, Moisan and Reiller [20] suggested a much stronger uptake, Wieland argued on the yet ill-defined aqueous speciation of Nb(V) in hyperalkaline systems (and consequently on the uptake mechanism) to select more conservative values. Ochs, Mallants and Wang [9] selected as best estimate R_d 5.0 • 10^4 L·kg^{-1} for all degradations stages of cement. This selection was based on the experimental data on Nb(V), but also considered the analogy with Sn(IV), for which the predominance of the anionic hydrolysis species $Sn(OH)_6^{2-}$ is foreseen under hyperalkaline conditions.

Isosaccharinic acid (ISA) is a polyhydroxocarboxylic acid forming upon degradation of cellulose in hyperalkaline conditions [25,26]. The formation of very stable complexes of ISA with actinides, lanthanides and transition metals is described in the literature [27–36], although less experimental evidence is available for transition metals as compared to the extensively studied actinide and lanthanide systems. The formation of stable aqueous complexes with ISA can expectedly result in a decreased uptake of radionuclides by cementitious materials, and thus deserves a close evaluation. A limited number of experimental studies have been dedicated to investigate the complexation of Nb(V) with organics ligands in aqueous systems, and virtually none targeting ISA. Fairbrother and co-workers investigated the complexation of Nb(V) with a number of carboxylic acids with alcohol groups in α-position, *i.e.* glycolic, lactic, malic and citric acids [37,38]. Although the main goal of the authors was of preparative character, they reported the formation of stable complexes involving the carboxylate and deprotonated α-alcohol groups. The authors also confirmed that the niobium complexes are formed by the coordination of the organic ligand to niobium and the completion of a five-membered ring by elimination of water. Although nothing is said about the thermodynamic stability of these complexes, the formation of analogous complexes can be envisaged for ISA. There is no established chemical analogue for pentavalent niobium, although Sn (IV) and Zr(IV) have been often considered in the literature to gain additional insight on the solution chemistry and sorption properties of Nb(V) [2,9,24]. The three elements/oxidation states share some similarities in terms of ionic radii ($r_{Sn^{4+}}$ 0.81 Å, $r_{Zr^{4+}}$ 0.84 Å, $r_{Nb^{5+}}$ 0.74 Å, all for a coordination number (CN) of 8) [39], and a strong hydrolysis that results in the predominance of negatively charged species in the high-pH conditions defined by cement, expectedly $Sn(OH)_6^{2-}$, $Zr(OH)_6^{2-}$ and $Nb(OH)_7^{2-}$. Kobayashi and co-workers recently studied the complexation of ISA and gluconate with Zr(IV) in alkaline to hyperalkaline conditions [34]. Based on their systematic solubility experiments, the authors proposed the formation of the aqueous complexes $Zr(OH)_4(ISA)_2^{2-}$ and $Zr(OH)_4(ISA)(ISA_{-H})^{3-}$, where ISA_{-H} corresponds to an ISA molecule with a deprotonated alcohol group. The latter species forms above pH ≈ 12, a pH-region in which the species $Zr(OH)_6^{2-}$ predominates in the absence of ISA. Although similar complexes can be envisaged for Nb(V), the impact of a stronger hydrolysis and smaller size on the stability of the complex/es forming remains to be experimentally assessed. No experimental studies on the impact of ISA

on the uptake of Nb(V) by cement are available in the literature, but this effect is well documented for other transition metals (*e.g.* Ni(II)), and especially for lanthanides and tetravalent actinides (*e.g.* Eu(III), Th(IV), Pu(IV)) [24,33,35,40–42]. In contrast to the strong impact of ISA on the uptake of An(IV), Wieland [24] indicated that "[…] *the influence of ISA on the uptake of Sn(IV) and Zr(IV) by HCP is expected to be weak due to limited thermodynamic stability of Zr(IV)-ISA and Sn(IV)-ISA complexes. Nevertheless, a possible effect on the Zr(IV) and Sn(IV) uptake by HCP is considered at the maximum ISA concentration of 3.7 • 10^{-3} M (sorption reduction factor 10)* […]". This assessment may need to be revisited in light of the new thermodynamic data reported by Kobayashi, Teshima, Sasaki and Kitamura [34] for the system Zr(IV)-ISA.

Stable chloride is expected in the repository originating from different sources, and may have an impact on the uptake of radionuclides especially at high concentrations. Wang and co-workers reported two main sources of stable chloride in radioactive waste, *i.e.* chloride associated with the production of concrete, and chloride originating from particular waste streams [2]. Whilst chloride concentration in the cement/concrete pore water is generally low (in the millimolar to sub-millimolar range), high concentrations of stable chloride (up to ≈4–5 M) have been described for specific waste streams containing evaporator concentrates (from nuclear power plants operation) [2]. The contribution of external sources to the overall stable chloride concentration is strongly dependent on the repository concept or location, and can be significantly increased in salt-based repositories (*e.g.* WIPP in the US) [43,44], specific clay formations characterized by intermediate ionic strength conditions (2 M < I < 6 M, *e.g.* Cretaceous argillites in Northern Germany or sedimentary bedrocks in the Canadian Shield) [45–48], or in repositories constructed in the vicinity of the sea, for which chloride concentrations in groundwater of up to 1.3 M have been reported [49,50]. Peiffert and co-workers conducted the only experimental study specifically targeting the impact of chloride on the solubility of Nb(V) [51]. The experiments were performed from undersaturation conditions using β-Nb_2O_5 in 1.0 m $NaClO_4$–NaCl solutions with 8 ≤ pH_m ≤ 14 and 0 ≤ [Cl^-] ≤ 0.5 m. Very similar results were obtained for $NaClO_4$–NaCl and pure $NaClO_4$ solutions, which led the authors to conclude that chloride has no effect on the solution chemistry of Nb(V) within the investigated boundary conditions. Baker and co-workers studied the uptake of Nb(V) by NRVB at pH 12.2 in saline systems with 0.5 M NaCl [23]. The R_d values reported by these authors are 5–10 times lower than distribution coefficients reported by [20] at similar pH values. Although one might be tempted to claim an effect of chloride/ionic strength to explain this discrepancy, the differences between the cementitious materials used in both studies prevent extracting any definitive conclusion.

In this context, this work aims at a quantitative evaluation of the Nb(V) uptake by cement CEM I in the degradation stage I. Besides the study of the binary system cement-Nb(V), the impact of ISA and chloride on the retention of niobium is also assessed on the basis of systematic sorption experiments with the ternary and quaternary systems cement-Nb(V)-ISA, cement-Nb(V)-Cl^- and cement-Nb(V)-ISA-Cl^-, respectively. This work is complemented by additional sorption studies on the binary systems cement-Nb(V) and cement-ISA [52], as well as by systematic solubility studies for the system Ca-Na-Nb(V)-H_2O with the aim of identifying the Nb(V) solid phases controlling the solubility in cementitious systems [53]. Because of the very low solubility limits of Nb(V) expected in the cement pore water (≈10^{-8}–10^{-6} M), the use of the ^{95}Nb isotope generated in a cyclotron facility through the nuclear reaction ^{nat}Zr(d,x) was considered in this study. Due to the short half-life of ^{95}Nb ($t_{1/2}$ 35.15 d), very low detection limits (≈10^{-14} M) can be achieved by gamma spectrometry.

2. Thermodynamic background: solubility, hydrolysis and complexation with ISA

An appropriate knowledge of the solubility and aqueous speciation of a given metal ion is advantageous for the correct design and interpretation of the corresponding sorption experiments. Niobium is only found in the +V oxidation state in aqueous systems, with lower oxidations states only forming below the border of water reduction, *i.e.* at (pe + pH) < 0 [14]. Table SD-1 in the Supplementary Data summarizes the thermodynamic data selected in the ThermoChimie database for Nb(V) hydrolysis species and solid compounds [54]. The main core of these data is selected from [51] (all hydrolysis species and solubility constant of Nb_2O_5(s)), whereas the solubility constant for the ternary solid phase $NaNbO_3$(cr) is selected from $\Delta_f H$ and $S°_m$ data reported in the NBS tables [55]. Thermodynamic data for the latter solid phase can be traced back to the review work by [56], who reported enthalpy and entropy data estimated for crystalline alkali metal oxides relevant to nuclear fuels, fission products and structural materials. The use of these thermodynamic data is disregarded in the context of the present study, because these crystalline phases are not expected to form in the aqueous systems of interest for this work.

Fig. 1a shows the fraction diagram of Nb(V) aqueous species within the pH-range 7 ≤ pH ≤ 14, as calculated with thermodynamic data summarized in Table SD-1. For comparative purposes, Fig. 1b and c show the fraction diagrams of Zr(IV) and Sn(IV) within the same pH-range calculated using thermodynamic data reported by Altmaier, Neck and Fanghanel [57] and selected in ThermoChimie [54], respectively (see Table SD-1 in the Supplementary Data). Note that the aqueous speciation of the three elements is analogous in the pH of interest for this work (pH 13.5), with the predominance of the hydrolysis species $Nb(OH)_7^{2-}$, $Zr(OH)_6^{2-}$ and $Sn(OH)_6^{2-}$. Notwithstanding, hydrolysis constants selected in ThermoChimie for Nb(V) are based on experimental studies up to pH ≈ 9, and thus the aqueous speciation of Nb(V) in hyperalkaline systems may differ from the current selection. Hence, Goiffon and co-workers proposed the formation of the monomeric species $NbO_2(OH)_4^{3-}$ at pH > 14.5 and [Nb] ≈ 10^{-4} M [58], whereas niobiate condensates (*e.g.* $Nb_4O_{16}^{12-}$) prevailed at higher Nb concentrations. The same monomeric species of Nb(V) may also prevail in systems with lower pH and Nb concentrations.

As discussed in the Introduction, the system Zr(IV)-ISA can be considered as a proxy to qualitatively assess the impact of ISA on the aqueous speciation of Nb(V) in alkaline to hyperalkaline pH conditions. Fig. 1d shows the aqueous speciation of Zr(IV) at pH constant 13.5 with 10^{-5} M ≤ $[ISA]_{tot}$ ≤ 0.1 M calculated using thermodynamic data reported in [34] (see Table SD-1 in the Supporting Data). The pH 13.5 was chosen for the calculations as representative of the cement in the degradation stage I investigated in this work. Although acknowledging the expected differences between the Nb(V)-ISA and Zr(IV)-ISA systems, these calculations predict a clear impact of ISA on the aqueous speciation of Nb(V) in the pH-range of interest for this work. Assuming that the Nb(V)-/Zr(IV)-ISA complexes do not sorb in cement, a decreased sorption of Nb(V) can be accordingly speculated above $[ISA]_{tot}$ ≈ 10^{-4} M.

3. Materials and methods

3.1. Chemicals and analytical methods

All solutions were prepared with purified water (Milli–Q academic, Millipore, 18.2 MΩ·cm) purged with Ar for >1 h in order to remove dissolved CO_2(g). Samples were prepared and equilibrated at T (22 ± 2) °C in a dedicated Ar-glove box with O_2 < 1 ppm. NaCl EMSURE, KCl EMSURE, NaOH Titrisol, KOH Titrisol and HCl Titrisol were obtained from Merck. Na_2SO_4, $CaCO_3$ and $Ca(OH)_2$, all of analytical grade, were purchased from Merck. KOH pellets (99.98%, metal base) were purchased from Alfa Aesar. $NbCl_5$ (99%) was obtained from Sigma-Aldrich. The zirconium foil (0.12 mm thick, 99.5% purity) used as target material for the production of ^{95}Nb was purchased from Alfa Aesar. DOWEX® (1 × 8, 200–400 mesh and 50 W × 8, 50–100 mesh) and UTEVA resins used for the separation of Zr and Nb were obtained by Sigma-Aldrich and TRISKEM international, respectively.

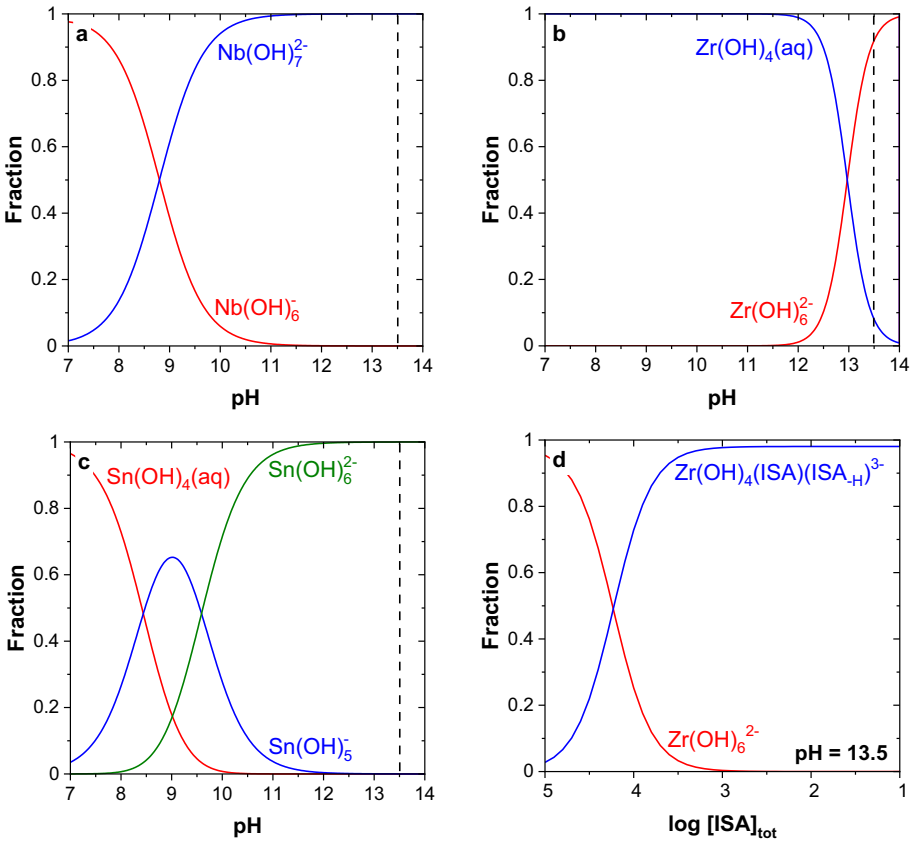

Fig. 1. Fraction diagrams of the systems (a) Nb(V)-H_2O, (b) Zr(IV)-H_2O and (c) Sn(IV)-H_2O calculated for the pH-range $7 \leq pH \leq 14$ using thermodynamic data selected in the ThermoChimie [54] database (Nb, Sn) or reported in Altmaier, Neck and Fanghanel [57] (Zr). (d) Fraction diagram of the system Zr(IV)-ISA calculated for $5 \leq \log [ISA]_{tot} \leq 1$ and pH = 13.5 using thermodynamic data reported in Kobayashi et al. [34]. All calculations performed at $[M]_{tot} = 10^{-9}$ M and $I = 0.5$ M. Dashed vertical lines indicate the pH of interest in this study, *i.e.* corresponding to HCP in the degradation stage I. All thermodynamic data summarized in Table SD-1 of the Supporting Data.

The α-isosaccharinic acid (ISA) used in this work was synthesized by L. Van Loon and M. Glaus (PSI-LES) in the lactone form, *i.e.* α-isosaccharino-1,4-lactone. The synthesis method used was previously described in Vercammen [59] as a slight modification of the original procedure described by Whistler and J.N. [60]. Elemental analysis of the crystals showed an excellent agreement in weight compared to pure ISA lactone (2 g). The ISA lactone was dissolved in 25 mL of a 0.1 M NaOH solution, and the resulting solution characterized by ^1H and ^{13}C nuclear magnetic resonance spectroscopy (NMR, Bruker Avance III 400 spectromete1.1r, operating at 400.18 MHz for ^1H and 100.63 MHz for ^{13}C). The ^1H NMR spectra confirmed the complete transformation of the lactone in the open chain form, as well as the purity of the final ISA product (see Fig. SD-1 in the Supporting Information).

The pH values were measured using combination pH electrodes ROSS Orion, with 3.0 M KCl as filling solution. Prior to the measurements the calibration of the electrode was performed using buffers (pH 1–12, Merck). The H^+ concentration in solutions with $[OH^-] > 0.03$ M was not measured experimentally but calculated instead using the conditional ion product of water.

Gamma spectrometry was used for the quantification of the active niobium isotopes. Measurements were performed using a high purity Germanium detector (61 mm × 46 mm, Mirion) with an energy resolution of 1.8 keV at 1.33 MeV and 0.875 keV at 122 keV. Samples were exchanged with an in-built auto-sampler (IMPROMAT, Belgium). The calibration range of the detector was 45–1800 keV, with an Eckert und Ziegler multi element standard used as calibration solution. The sample geometry was defined by 10 mL PP flasks (Kautex, a Textron Company) with total sample volume of 10 mL. The isotopes ^{91m}Nb ($t_{1/2}$ 64.0 days), ^{92m}Nb ($t_{1/2}$ 10.16 days) and ^{95}Nb ($t_{1/2}$ 35.15 days) were quantified following the gamma lines 1205.0 keV (3.4 photons per 100 disintegrations), 934.5 keV (95.5 photons per 100 disintegrations) and 765.82 keV (99.0 photons per 100 disintegrations), respectively. Measuring times ranged between 1 and 4 h, depending on the activity of the sample. The detection limits for these isotopes and gamma lines were ≈2.2 Bq·mL^{-1} (^{91m}Nb), ≈1.0 Bq·mL^{-1} (^{92m}Nb) and ≈0.1 Bq·mL^{-1} (^{95}Nb), depending on the measuring time. Considering the internal dilution steps, these values translate into detection limits of ≈$5 \cdot 10^{-15}$ M (^{91m}Nb), $2 \cdot 10^{-15}$ M (^{92m}Nb) and $1 \cdot 10^{-16}$ M (^{95}Nb).

3.2. Production of ^{95}Nb isotope

The nuclear (d,x) reaction on a Zr target with natural isotopic composition was used to produce ^{95}Nb (n.c.a.) at a cyclotron Cyclone 18/9® (IBA RadioPharma Solutions, Belgium). A Zr foil with natural isotopic composition (Ø 12 mm × 127 µm, AlfaAesar, Germany) was bombarded with 9 MeV deuterons for 665 µAh using the COSTIS target station (IBA RadioPharma Solutions, Belgium) mounted at a beam line at port 3 of the cyclotron (see Fig. SD-3 in the Supplementary Data). The target was aligned perpendicular to the beam axis, 12 mm was the diameter of the beam spot. The target was cooled with He in the front and water at the backside.

The target capsule was stored for 4 days after completing the irradiation to allow unwanted short lived radionuclides to decay. Afterwards the capsule was opened and the irradiated Zr foil transferred to γ-spectrometry. The obtained spectrum is dominated by ^{91m}Nb, ^{92m}Nb, ^{95}Nb, ^{95m}Nb and ^{95}Zr (see Fig. SD-5 in the Supplementary Data). Although ^{95}Nb was the main isotope considered for the quantification of Nb in the sorption experiments, ^{91m}Nb (with similar activity as ^{95}Nb after irradiation but a far less probable gamma line, see Section 3.1) was also detected in those experiments with higher activity remaining in solution. The shorter-lived isotope ^{92m}Nb was present with the highest activity directly after the irradiation of the Zr target (2–3 times the activity of ^{95}Nb or ^{91m}Nb) but could hardly be observed in any of the sorption experiments, which were conducted within the time window ≈35–140 days after finalizing the irradiation process.

3.3. Separation of Zr and Nb. Preparation of the ^{95}Nb stock solution

The Nb stock solution was obtained by dissolution of the irradiated Zr foil and later separation of zirconium and niobium in the aqueous phase. The dissolution and separation processes were based on a modified version of the separation schemes reported previously in the literature [61,62]. In particular, the original schemes were modified to avoid the use of high concentrations of oxalic acid in the separation process, which may later interfere in the sorption experiments with Nb and ISA. The complete separation procedure is summarized in the scheme in Fig. SD-6 of the Supporting Data.

The irradiated Zr target containing several isotopes of Nb and Zr (^{91m}Nb, ^{92m}Nb, ^{95}Nb, ^{95m}Nb, ^{95}Zr as well as stable isotope ^{93}Zr) was dissolved in 1.5 mL H_2O + 1.5 mL 48% HF. After the total dissolution of the target, additional 3 mL of 48% HF were spiked to the solution containing the Zr-Nb mixture. 300 mg of the cation exchange resin DOWEX® 50 W × 8 were soaked in 2 mL of 48% HF for approximately half an hour, transferred to a 2 mL PP + PE column, and washed with additional 2 mL 48% HF. The 6 mL of the Zr-Nb solution were passed through the resin, which was washed with additional 3 mL of concentrated HF. Divalent and trivalent metal cations, as well as colloids and undissolved particles were retained by the column, whereas the anionic species NbF_x^{5-x} (with $x \geq 7$) [63–66] remained in solution and were collected in the eluate.

In order to separate the bulk amount of Zr, 600 mg of the anion exchange resin DOWEX® 1 × 8 were soaked in 4 mL of 48% HF for about half an hour, placed in the column and washed with 4 mL of concentrated HF. Approximately 9 mL of the elute collected from the previous step were transferred to the column. DOWEX® 1 × 8 has been shown to have a high affinity towards the anionic Nb(V)-F species prevailing in concentrated HF solutions compared to Zr(IV)-F [67], and thus the former anionic species were retained in the resin whilst the bulk of Zr was discarded in the eluate. Residues of Zr were eluted by washing the column with additional 18 mL of 48% HF. The resin was washed with 2 mL of 1 M HCl, and Nb was eluted with 2 mL of 6 M HCl/1% H_2O_2. The elute containing Nb was heated at 120 °C for 5 min to remove the H_2O_2, and 2.1 mL of 37% HCl were added to the remaining solution.

The UTEVA resin (Uranium and TEtraValent Actinides, with the extractant dipentyl pentylphosphonate coated onto an inert support) is primarily used for the separation of U(VI) and An(IV) [68,69], although its applications extend to many other metal ions and radionuclides, including Nb and Zr [62,70]. 300 mg of UTEVA resin were soaked in 2 mL 37% HCl, transferred to a 2 mL PP + PE column and washed with additional 2 mL 37% HCl. The eluate collected from the last separation step was passed through the column, followed by 18 mL of 5.5 M HCl. The acid concentration was optimized in this work to achieve the highest selectivity for Nb(V), whereas the remaining Zr(IV) traces were discarded with the eluate. The Nb(V) retained in the UTEVA resin was eluted with 18 mL of 2 M HCl, and the eluate was evaporated to dryness. The residue was dissolved in 10 mL of 8 M HNO_3, cooked and slowly evaporated to dryness in order to degrade the organics in solution that may have leached from the resins. The final Nb(V) stock solution was obtained with the dissolution of the residue in 10 mL 2% HNO_3. The concentrations of Nb and Zr in the stock solution were quantified by gamma spectrometry and ICP-MS, respectively, resulting in $[Nb]_{tot}$ $(2.5 \pm 0.3) \cdot 10^{-9}$ M and $[Zr]_{tot} \leq 10^{-8}$ M (detection limit of ICP–MS at the conditions of the experiment), with $[^{95}Nb]$ $(1.5 \pm 0.12) \cdot 10^{-9}$ M (1.23 ± 0.1 MBq·mL^{-1}), $[^{91m}Nb]$ $(1.0 \pm 0.01) \cdot 10^{-9}$ M (1.0 ± 0.01 MBq·mL^{-1}), and $[^{95}Zr] \leq 3 \cdot 10^{-16}$ M ($\leq$0.12 Bq·mL^{-1}, detection limit of gamma counting in the conditions of the experiment). The yield of ^{95}Nb obtained in the dissolution and separation processes was calculated as (14 ± 1)%. The low yield obtained compared to previous studies is expectedly related to the discard of oxalate in the separation process.

Due to the very short half-life of the ^{95}Nb isotope (35.15 d) the preparation of the final solution in 2% HNO_3 was considered as reference time (t 0) for the calculation of the Nb concentrations along the sorption experiments.

3.4. Preparation and characterization of HCP and cement pore water

Cement CEM I 52,5 N SR0 CE PM-CP2 NF provided by ONDRAF-NIRAS was hydrated by mixing of 690 g of cement powder with 316 g of water, *i.e.* with a water-to-cement ratio (w/c) of 0.46. After two days of setting, the monolith was immersed in water and cured for approximately 2.5 months. Both setting and curing were performed in a glovebox under Ar atmosphere to avoid the carbonation of the cement paste. After terminating the curing process, the outer layer of the cement monolith (≈2.5 mm) was cut to remove any altered surface. This procedure was performed under inert atmosphere in a glove bag constantly purged with Ar. The resulting material was transferred to an Ar glovebox, where it was ground with manual crushing, followed by milling and sieving with a Pulverisette 0 equipment (Fritsch GmbH). The milling was performed with tungsten-carbide ball whereas a sieve with 63 μm mesh size was used for the sieving. The final powder (435 g in total) was obtained after milling and sieving the complete monolith down to 63 μm, *i.e.* particles of larger size were repeatedly milled until all the cement powder passed through the 63 μm sieve. This precaution was taken to avoid any size fractionation of the different cement phases that may have led to less representative sorption data. The initial cement clinker and the hydrated cement paste powder were characterized by X-ray powder diffraction (XRD) and scanning electron microscope (SEM). XRD patterns were collected with a Bruker D8 Advance X-Ray powder diffractometer (Cu anode) at 2θ 10–100° with incremental steps of 0.008° and a measurement time of 0.1 s per step. SEM images were taken using a Quanta 650 FEG apparatus.

Young cement pore water (YCWCa) representative of cement CEM I in the degradation stage I was prepared following the modified version of the recipe developed by SCK-CEN [71]. Briefly, 136 g of 1.0 M NaOH, 370 g of 1.0 M KOH, 0.284 g Na_2SO_4, 0.03 g $CaCO_3$ and 0.02 g $Ca(OH)_2$ were dissolved in 1 L of Milli-Q water targeting the following composition: pH 13.5, [Na] 0.14 M, [K] 0.37 M, [Ca] $4.8 \cdot 10^{-4}$ M, [Si] $4 \cdot 10^{-4}$ M, $[SO_4^{2-}]$ $2 \cdot 10^{-3}$ M and $[CO_3^{2-}]$ $3 \cdot 10^{-4}$ M. Preliminary measurements of the pore water composition after equilibrating the YCWCa with cement showed a systematic increase in the concentration of Ca to $\approx 1.4 \cdot 10^{-3}$ M. For this reason and to avoid the dissolution of portlandite in the investigated cement systems, the concentration of calcium in YCWCa was increased to $1.4 \cdot 10^{-3}$ M. This calcium concentration is in line with data reported from the squeezing of ordinary Portland cement reported elsewhere [72]. The evolution of the pore water composition (concentrations of Na, K, Ca) after equilibration with cement was characterized by inductively coupled plasma-optical emission spectroscopy (ICP-OES). Aliquots of the pore water (100–250 μL) were diluted in 2% HNO_3 after ultrafiltration with 10 kD filters (2–3 nm cut-off Nanosep®, Pall Life Sciences) to separate colloids of suspended particles. The concentration of chloride leached from the cement after equilibration with YCWCa was quantified by ion chromatography using a ICS-3000 (Thermo Scientific™) equipment.

The content of ^{93}Nb was characterized in both HCP and the YCWCa equilibrated with HCP. A fraction of 200 mg of HCP was mixed with 1.5 g of KOH pellets in a Pt/Au crucible, and heated up to 390 °C for 15 min on a hot plate to melt the mixture. The crucible was placed in a polypropylene beaker, and Milli-Q water was added under magnetic stirring to wash out the complete amount of dissolved mixture from the crucible. 30 mL of 32% HCl were added to the beaker and a clear solution was obtained. The solution was transferred to a 250 mL glass volumetric flask, and the remaining volume was filled with Milli-Q water. The concentration of Nb in the resulting solution was quantified by ICP-MS after a dilution 1:10.

20 mL of YCWCa pore water were contacted with 20 mg of HCP (*i.e.* at S:L 1 g·L^{-1}) for two months. An aliquot of the supernatant was separated by 10 kDa ultrafiltration, and the concentration of ^{93}Nb

leached from the cement was quantified by ICP-MS.

3.5. Solubility of Nb(V) in cement pore water and solid phase characterization

A 1.3 • 10^{-3} M Nb(V) stock solution was prepared by dissolution of $NbCl_5$ in 0.2 M NaOH. Appropriate volumes of the stock solutions were added to YCWCa to set the initial Nb concentration to 1.0 • 10^{-5}, 1.0 • 10^{-4}, and 5.0 • 10^{-4} M. A white precipitate was observed in all samples shortly after the addition (in 2–3 min) of Nb(V) to YCWCa. After contact times of t 32, 57 and 200 d, aliquots of samples were taken and the aqueous phase was separated by 10 kDa ultrafiltration. The filtered aqueous phase was diluted in 2% HNO_3 and the Nb(V) concentration was determined by ICP-MS.

After t 200 days, the solid phase in the solubility sample with [Nb(V)]$_0$ 5.0 • 10^{-4} M was separated by centrifugation, washed 5 times with ethanol, dried under Ar atmosphere and characterized by XRD analysis at 2θ 10–90° with incremental steps of 0.013° and a measurement time of 1.5 s per step.

3.6. Sorption experiments: binary, ternary and quaternary systems

All experiments were performed in HDPE vials (Zinsser Analytic) with a total volume of 4–20 mL, depending upon S:L ratio, $[Nb]_0$ and $[ISA]_{tot}$. All samples were equilibrated under constant agitation using an orbital shaker VXR basic Vibrax (IKA). The binary system cement-Nb(V) was investigated with a comprehensive series of sorption experiments with 0.1 g·L^{-1} ≤ S:L ≤ 50 g·L^{-1} and 10^{-13} M ≤ $[Nb]_0$ ≤ 10^{-7} M. The broad range of initial Nb concentrations in the YCWCa was achieved using a combination of active (^{95}Nb) and inactive (^{93}Nb) isotopes. Note that these concentration values do not account for the possible leaching of ^{93}Nb from the cement.

In a second step, the ternary systems cement-Nb(V)-ISA and cement-Nb(V)-Cl^- were investigated under variation of the initial ISA and Cl^- concentrations, *i.e.* 10^{-5} M ≤ $[ISA]_{tot}$ ≤ 0.1 M and 10^{-3} M ≤ $[Cl^-]_{tot}$ ≤ 0.1 M, respectively. Experiments in the presence of ISA were conducted following two different orders of addition of the individual components: "(*cement* + *Nb*) + *ISA*" and "(*Nb* + *ISA*) + *cement*". Previous studies with the ternary system cement-Pu-ISA have shown that the uptake in the system "(*RN* + *ISA*) + *cement*" is kinetically hindered and often results in significantly lower distribution coefficients [33]. In a final step, the quaternary system cement-Nb(V)-ISA-Cl^- was investigated following the order of addition "(*Nb* + *cement* + Cl^-) + *ISA*", with $[ISA]_{tot}$ constant 0.1 M and 10^{-5} M ≤ $[Cl^-]_{tot}$ ≤ 1.0 M. The experimental conditions of all investigated systems are summarized in Table 1.

After the given contact time as defined in Table 1, an aliquot of the supernatant (0.5 to 5 mL) of each sample was centrifuged for 3 min using 10 kD filters for the separation of colloids and suspended particles. A given volume of the filtrate was diluted in 2% ultrapure HNO_3 (dilution factors of 1:2 to 1:20, depending upon initial Nb concentration), and both ^{95}Nb and ^{91m}Nb were quantified by gamma spectrometry. The uncertainty of the gamma measurements was ±5–10%, whereas the detection limit of the method was ≈1 • 10^{-16} M for ^{95}Nb and ≈5 • 10^{-15} M for ^{91m}Nb (considering also the dilution factors used for sample preparation). The possible sorption of Nb(V) on the filters and the HDPE vessels was evaluated with a series of targeted experiments with 10^{-15} M ≤ $[Nb]_{tot}$ ≤ 10^{-12} M, where $[Nb]_{tot}$ [^{91m}Nb] + [^{93}Nb] + [^{95}Nb]. No significant sorption (<5%) on the vessels was observed, whereas approximately 10% of Nb was sorbed by the filters, independently of the initial Nb concentration. This effect was corrected in the calculation of the Nb concentrations in the sorption experiments. For the samples containing active (^{95}Nb) and inactive (^{93}Nb) niobium in the absence of ISA, an aliquot of the supernatant was separated by 10 kDa ultrafiltration, and the concentration of ^{93}Nb was quantified by ICP-MS.

The uptake of Nb(V) by HCP was evaluated in terms of distribution ratios, R_d (in L·kg^{-1}), as a function of time (kinetic experiments), $[ISA]_{tot}$ and $[Cl^-]_{tot}$. R_d values were calculated as the ratio of niobium concentration in the solid ($[Nb]_{solid}$, in mol·kg^{-1}) and aqueous ($[Nb]_{aq}$, in M) phases:

$$R_d \quad \frac{[Nb]_{solid}}{[Nb]_{aq}} \bullet \frac{V}{m} \quad \frac{[Nb]_0 \quad [Nb]_{aq}}{[Nb]_{aq}} \bullet \frac{V}{m} \tag{1}$$

where $[Nb]_0$ is the initial niobium concentration, V is the volume of the sample (L) and m is the mass of cement used in the experiment (kg). Uncertainties in the R_d values were calculated as three times the standard deviation of repeated measurements. For those sample for which only single measurements were available, average uncertainties of ±0.3 (experiments with only ^{95}Nb) and ± 0.2 (experiments with ^{95}Nb and ^{93}Nb) were considered.

4. Results and discussions

4.1. Characterization of HCP and cement pore water

Fig. 2 shows the background-subtracted XRD diffractograms collected for the original cement clinker and the HCP, as compared to reference data available in the Joint Committee on Powder Diffraction Standards database [73]. Features observed for the clinker material agree well with reference data reported for alite (3CaO·SiO_2 (C_3S), harturite, PDF 86-0402), belite (2CaO·SiO_2 (C_2S), larnite, PDF 09-0351) and calcium aluminoferrite (4CaO·$Al_nFe_{2-n}O_3$ (C_4AF), brownmillerite, PDF 30-0226). These phases are acknowledged as main constituents in standard Portland cement clinkers [74], and are consistent with specifications reported by the producer of the cement material used in this work (58% C_3S, 24% C_2S, 16% C_4AF and 2% "others"). The diffractogram collected for the hydrated HCP shows mainly the patterns corresponding to portlandite ($Ca(OH)_2$, PDF 04-07339). Other minor reflections can be tentatively assigned to calcium silicate hydrate phases (Ca_3SiO_5, PDF 70-1846), ettringite ($Ca_6Al_2(SO_4)_3(OH)_{12}$·$26H_2O$, PDF 37-1476) or calcium aluminoferrite (brownmillerite, PDF 30-0226). These observations are in line with the main phases expected for the hydrated Portland cement [72,74]. Note that the absence of any of the patterns corresponding to alite and belite reflects that the final product is fully hydrated. The different morphology of the original clinker material and the hydrated HCP is also reflected in the SEM images shown in

Table 1
Experimental conditions adopted in the sorption experiments with the binary (cement-Nb(V)), ternary (cement-Nb(V)-ISA, cement-Nb(V)-Cl) and quaternary systems (cement-Nb(V)-ISA-Cl) investigated in this work.

System	Type of experiment	Time (days)	S:L [g·L ^{1}]	[^{93}Nb]$_0$ [M]	[^{95}Nb]$_0$ [M]/A[^{95}Nb]$_0$ [Bq/mL]	$[ISA]_{tot}$ [M]	$[Cl^-]_{tot}$ [M]
Cement-Nb(V)	Kinetics	1–30	1, 10		1.1–4.7 10 ^{11}/1.5–6.5 • 10^3	–	–
	Effect of S/L	1–30	1, 5, 10		1.1–4.7 10 ^{11}/1.5–6.5 • 10^3	–	–
	Variation of $[Nb]_0$	1–30	1	10 ^{7}–3 • 10 ^{10}	1.1–4.7 10 ^{11}/1.5–6.5 • 10^3	–	–
Cement-Nb(V)-ISA	Variation of $[Nb]_0$	7–54	1	10 ^{7}–3 • 10 ^{10}	9.1 • 10 ^{13}–1.1 10 ^{11}/1.3 • 10^2–1.5 • 10^3	0.1	–
	Effect of $[ISA]_{tot}$	7–54	1		1.1 10 ^{11}/1.5 • 10^3	10 ^{5} – 0.1	–
	Order of addition	7–54	1		1.1 10 ^{11}/1.5 • 10^3	10 ^{5} – 0.1	
Cement-Nb(V)-Cl	Effect of $[Cl^-]_{tot}$	4–12	0.1	–	4.5 10 ^{12}/6.3 • 10^2	–	10 ^{3}–0.1
Cement-Nb(V)-ISA-Cl	Effect of $[Cl^-]_{tot}$	20	1	–	1.8 10 ^{12}/2.5 • 10^2	0.1	10 ^{5}–1.0

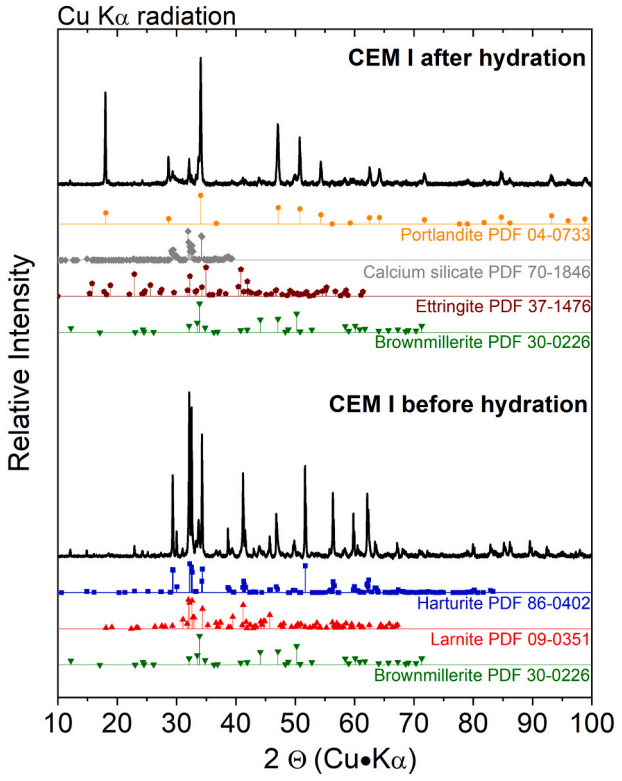

Fig. 2. XRD patterns collected in the present work for the original clinker and the hydrated cement. Reference data shown for harturite ($3CaO{\cdot}SiO_2$, PDF 86-0402), larnite ($2CaO{\cdot}SiO_2$, PDF 09-0351), calcium silicate hydrate (Ca_3SiO_5, PDF 70-1846), portlandite ($Ca(OH)_2$, PDF 04-0733); ettringite ($Ca_6Al_2(SO_4)_3(OH)_{12}{\cdot}26H_2O$; PDF 37-1476) and brownmillerite ($4CaO{\cdot}Al_nFe_{2-n}O_3$ PDF 04-0733).

Fig. SD-7 as Supplementary Data.

Table SD-2 in the Supplementary Data summarizes the composition of the artificial cement pore water before and after contacting the HCP with S:L ratios of 2, 5, 10 and 50 $g{\cdot}L^{-1}$. The table confirms that no significant changes in the pore water composition took place before and after the equilibration with the hydrated cement, thus supporting that the considered YCWCa represents well the investigated cement system. Note that no differences in the pore water composition are observed either for the different S:L ratios evaluated.

The concentrations of niobium in HCP and YCWCa equilibrated with HCP were quantified as (3.1 ± 0.3) ppm (*i.e.* (3.3 ± 0.3) • 10^{-5} $mol{\cdot}kg^{-1}$) and (8 ± 3) • 10^{-10} M, respectively. None of the previous experimental studies dedicated to the uptake of niobium by cement has reported the content of natural Nb in the HCP, but values reported in Ochs et al. [9] for three cement types proposed for use in the Dessel repository, CEM I, CEM III-B and CEM III-C ranged between 5.1 and 7.6 ppm. Tachi and co-workers determined [Nb] 1.29 • 10^{-9} M in the pore water of a HCP equilibrated with artificial cement pore water at pH 12.9 [77]. These observations underline the intrinsic content of niobium in pristine HCP and cement pore water, which accordingly need to be accounted for a correct interpretation of the mechanisms driving the uptake of Nb by cement.

4.2. Solubility of Nb(V) in YCWCa

Oversaturation solubility experiments in YCWCa resulted in [Nb(V)] 2 • 10^{-6}–7 • 10^{-8} M independently of the initial niobium concentration, *i.e.* $[Nb(V)]_0$ 1.0 • 10^{-5}, 1.0 • 10^{-4} and 5.0 • 10^{-4} M. The drop in the niobium concentration was accompanied by the formation of a white precipitate, and equilibrium conditions were attained after ≈57 days. The solubility limit experimentally determined in YCWCa was considered as input parameter for the design of the sorption experiments.

Niobium concentrations measured in the present work are not consistent with a solubility-control by Na-niobiate solid phases previously described in the literature, *e.g.* $Na_8Nb_6O_{19}{\cdot}13H_2O$(s) or $Na_7HNb_6O_{19}{\cdot}15H_2O$(s), for which significantly higher niobium concentrations (in the millimolar range) have been reported [17,18]. On the other hand, solubility data determined in this work are slightly higher but still in line with niobium concentrations reported in hyperalkaline systems containing calcium [19,21]. The higher pH values investigated in this work may partially explain the observed differences.

Fig. 3 represents the background-subtracted XRD diffractogram of the white Nb(V) solid phase precipitated in YCWCa. Patterns of the Nb(V) precipitate are in excellent agreement with reference data reported for a cubic pyrochlore-structure type Ca-Nb(V) oxide ($Ca_2Nb_2O_7$(cr), PDF 81-0841). Quantitative chemical analysis conducted for these solid phases confirm the presence of Ca and absence of Na, thus underpinning the XRD analysis in the present work. Previous solubility studies with Nb(V) in Ca-containing alkaline systems have reported the possible formation of the poorly crystalline phases $CaNb_2O_6{\cdot}xH_2O$(s) [19] and $CaNb_4O_{11}{\cdot}8H_2O$(s) (hochelagaite) [21], although the univocal assignment of the solid phase controlling the solubility was not achieved. We note that the three solid phases ($Ca_2Nb_2O_7$(cr), $CaNb_2O_6$(cr) and $CaNb_4O_{11}{\cdot}8H_2O$(cr)) share a main reflection at 2Θ ≈ 29.6° (see Fig. 3), which may lead to an incorrect assignment of the XRD patterns in poorly crystalline solid phases. The clear reflections observed in this work at 2Θ ≈ 14.7, 28.3, 29.6, 34.3,

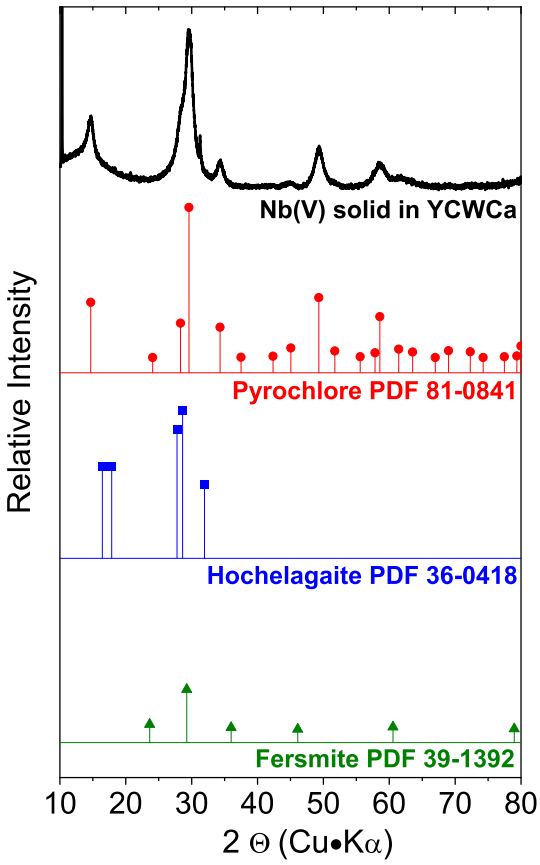

Fig. 3. XRD patterns collected in the present work for the Nb(V) solid precipitated in YCWCa. Major lines (relative normalized intensity > 0.15) of reference data shown for pyrochlore ($Ca_2Nb_2O_7$(cr), PDF 81-0841), hochelagaite ($CaNb_4O_{11}{\cdot}8H_2O$(cr), PDF 36-0418), and fersmite ($CaNb_2O_6$(cr), PDF 39-1392).

49.3 and 58.6° strongly support the predominance of a pyrochlore phase in YCWCa. An on-going solubility study at KIT–INE on the solid phases controlling the solubility of Nb(V) in hyperalkaline systems containing Ca ($10 \leq pH \leq 13$, $1 \cdot 10^{-5}$ M $\leq$ [Ca] $\leq$ 0.01 M) including a multi-method characterization of the solid phases will provide definitive insights on this elusive topic [53].

4.3. Uptake of Nb(V) by HCP in the absence of ISA

Sorption kinetics were investigated using only active niobium with [^{95}Nb] $4.7 \cdot 10^{-11}$ M (experiments with S:L 1 g·L^{-1}) and $1.1 \cdot 10^{-11}$ M (experiments with S:L 10 g·L^{-1}). Fig. 4 shows the uptake of Nb(V) (expressed as log R_d) at t 1, 2, 7 and 30 days. The results confirm fast sorption kinetics, *i.e.* equilibrium conditions were attained after only 2 days. Very strong sorption was observed in both kinetic experiments, with log $R_d \approx$ 6–7 (R_d in L·kg^{-1}). Experimental data suggests also the decrease of log R_d with increasing S:L ratio, although equilibrium values determined for both systems almost overlap when considering the corresponding uncertainties. Note that a decrease in R_d values with increasing S:L ratios was observed in previous sorption studies involving radionuclides and cement, although the mechanism behind this effect is not yet understood [8,9,75,76]. The fast uptake observed in this work for Nb(V) is in line with the sorption kinetics reported for other strongly sorbing metal ions, *e.g.* Th(IV) or Tc(IV) [20,41].

Fig. 5 compares log R_d values determined in this work for the uptake of ^{95}Nb(V) by HCP (S:L 1–10 g·L^{-1}, pH 13.5), with data reported in the literature for Nb(V) and HCP (S:L 5–40 g·L^{-1}, pH 11.8) [22], NRVB (S:L 20 g·L^{-1}, pH 12.1) [23], HCP and C-S-H phases (S:L 0.5 g·L^{-1}, pH 10–12.5) [20], as well as HCP (S:L 10 g·L^{-1}, pH 12.5 and 12.9). Most of our data are grouped at log $R_d \approx$ 5–5.5, in excellent agreement with the distribution coefficients reported by Baker et al. and Pointeau et al. for NRVB, HCP and C-S-H phases. We do not have a definitive explanation for the very high log R_d values (≈7) obtained for the sample containing only ^{95}Nb at S:L 1 g·L^{-1} (blue symbol in Fig. 5), but note that all other samples at S:L 1 g·L^{-1} containing both ^{95}Nb and ^{93}Nb (with $[Nb]_{tot}$ $1.0 \cdot 10^{-7}$, $1.0 \cdot 10^{-8}$ and $3.4 \cdot 10^{-10}$ M) show consistent values with log R_d (5.1 ± 0.2).

The three studies showing the highest log R_d values (this work, [23] and [20]) are characterized by the use of the short-lived isotope ^{95}Nb ($t_{1/2}$ 35.15 days), which allows the use/quantification of very low residual Nb concentrations and thus avoids any interference caused by solubility phenomena. The low log R_d values reported by Pilkington and Stone [22] are expectedly due to the very high initial concentration

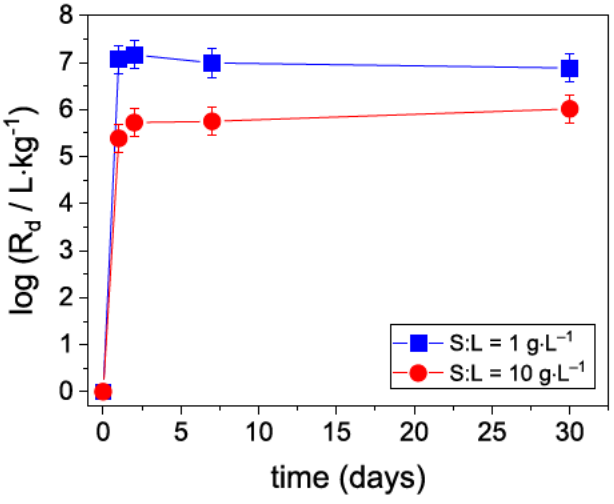

Fig. 4. Kinetics of ^{95}Nb(V) uptake by HCP in the degradation stage I (YCWCa). Initial Nb(V) concentrations are $4.7 \cdot 10^{-11}$ (S:L = 1 g·L^{-1}) and $1.1 \cdot 10^{-11}$ M (S:L = 10 g·L^{-1}). R_d values expressed in L·kg^{-1}.

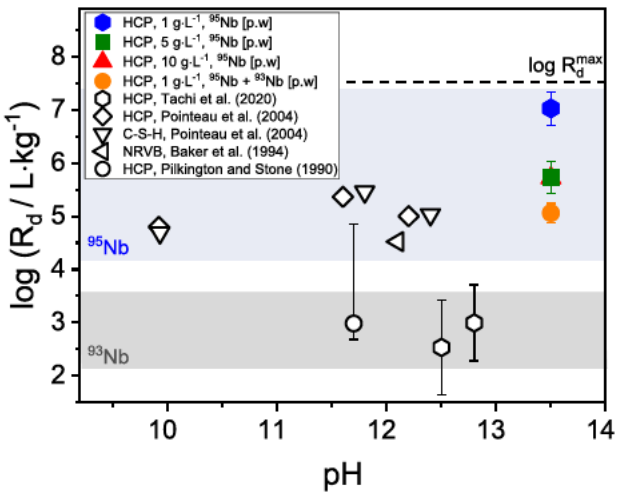

Fig. 5. Distribution coefficients determined in this work for the uptake of Nb (V) by HCP in the degradation stage I, or reported in the literature HCP [22], NRVB [23], or HCP and C-S-H [20]. The two regions highlighted in the figure mark the experiments performed with ^{93}Nb or ^{95}Nb. The term [p.w.] stands for present work.

of inactive ^{93}Nb ($5.3 \cdot 10^{-3}$ M), which must have resulted in a solubility-control of the Nb(V) concentration in solution. Tachi, Suyama and Mihara [77] used the inactive isotope ^{93}Nb to investigate the uptake of Nb(V) by HCP in distilled water (pH 12.5) and artificial pore water (pH 12.8–12.9). The authors used low initial niobium concentrations ($[^{93}Nb]_0$ $8.1 \cdot 10^{-9}$–$5.7 \cdot 10^{-8}$ M), and thus their results are expectedly not affected by solubility phenomena.

The review work by Wieland [24] recommended the use of the sorption value log R_d 3 (with R_d in L·kg^{-1}) for the uptake of Nb(V) by HCP in the three degradation stages of cement (I, II and III), although acknowledged that there is ample evidence that the distribution coefficients could be much higher. Accounting for experimental data reported by [20,22,23], the review work by Ochs and co-workers selected higher distribution coefficient values, with best estimate, upper and lower limits reported as log R_d 4.7, 6 and 3, respectively [9]. Our experimental results are in line with the best estimate and upper limit proposed by the latter authors, whilst the discussion above highlights that discrepancies in data available in the literature are probably related with systematic differences between sorption experiments using natural ^{93}Nb or radioactive ^{95}Nb.

The identification of ^{93}Nb in the HCP represents a change of paradigm in the interpretation of the mechanism/s driving the uptake of Nb by cement and, by extension, imposes a different perspective for the evaluation of sorption data in Fig. 5. As in the case of nickel, the presence of natural ^{93}Nb in the HCP implies that isotopic exchange needs to be considered as plausible mechanism for the uptake of other niobium isotopes (^{95}Nb in this work, ^{94}Nb in the repository) by cement. Pointeau and co-workers reported a strong sorption of ^{95}Nb by C-S-H phases of different Ca:Si ratios ([20]; see Fig. 5), which supports that these phases must be considered as one of the main sinks of niobium in cement. Although it can be speculated that sparingly soluble Ca-Nb(V) oxo/hydroxide compound/s may represent the main inventory of ^{93}Nb in HCP and thus be the main source for the isotopic exchange with ^{95}Nb/^{94}Nb, both the uptake by C-S-H phases and isotopic exchange with yet undefined ^{93}Nb solid phases in HCP must be considered in the discussion of the retention processes of radioactive Nb in cementitious systems.

Assuming the ubiquitous presence of ^{93}Nb in most cement formulations, experimental data in sorption studies using only ^{93}Nb must be reinterpreted considering greater values of $[Nb]_{solid}$ at equilibrium. Significantly higher log R_d values (in line with sorption data for ^{95}Nb) are accordingly calculated from experimental data with ^{93}Nb reported in

Tachi et al. [77] and considering a concentration of ^{93}Nb in the pristine HCP in the range of 3 to 8 ppm. Hence, the consideration of ^{93}Nb in HCP leads to a more consistent explanation of the available sorption data with both ^{93}Nb and ^{95}Nb.

As previously considered for nickel [78], the partition coefficient (α) can be used to describe the isotopic distribution of ^{95}Nb between the HCP and the cement pore water:

$$\alpha \quad \frac{\left(n_{solid,^{95}Nb}/n_{solid,^{93}Nb}\right)}{\left(n_{aq,^{95}Nb}/n_{aq,^{93}Nb}\right)} \quad \frac{R_{d,^{95}Nb}}{R_{d,^{93}Nb}} \qquad (2)$$

where $n_{solid,^{95}Nb}$ and $n_{solid,^{93}Nb}$ are the number of mols of ^{95}Nb and ^{93}Nb in HCP, $n_{aq,^{95}Nb}$ and $n_{aq,^{93}Nb}$ denote the number of mols of ^{95}Nb and ^{93}Nb in the cement pore water, and $R_{d,^{95}Nb}$ and $R_{d,^{93}Nb}$ are the distribution coefficients of ^{95}Nb and ^{93}Nb, respectively. From Eq. (2), it appears that α approaches 1 if the total inventory of ^{93}Nb in HCP is accessible to isotopic exchange. Measurements of ^{93}Nb in sorption samples containing both ^{93}Nb and ^{95}Nb resulted in concentration values below the detection limit of ICP-MS, *i.e.* $<8.6 \cdot 10^{-9}$ M, and thus the calculation of $R_{d,^{93}Nb}$ (and by extension the calculation of α) was not possible for these samples. The values of $[^{93}Nb]_{solid}$ determined in pristine HCP and $[^{93}Nb]_{aq}$ measured in the cement pore water (see Section 4.1) can be used to calculate an approximation of the distribution coefficient for ^{93}Nb, *i.e.* log $R_{d,^{93}Nb}$ (4.6 ± 0.2). The combination of this value with log $R_{d,^{95}Nb}$ (5.1 ± 0.2) as determined in this work for samples containing both ^{93}Nb and ^{95}Nb results in α values ranging between 1 and 6. Whilst α 1 indicates the full availability of ^{93}Nb in pristine HCP for isotopic exchange with ^{95}Nb, values of $\alpha > 1$ are meaningless and may hint that isotopic exchange is not the main/only uptake mechanism of Nb in cement. This hypothesis is in line with the expected strong uptake of Nb(V) by C-S-H phases as described by Pointeau and co-workers. Future efforts in a second phase of this project will target also the accurate quantification of $R_{d,^{93}Nb}$ both in HCP and in C-S-H phases.

The discussion of isotopic exchange *vs.* sorption on C-S-H phases as possible mechanisms for the uptake of ^{95}Nb/^{94}Nb requires also insights on the "dimension" of the corresponding "reservoirs". Hence, whilst the content of ^{93}Nb in HCP available for isotopic exchange is limited to $(3–8)\cdot10^{-5}$ mol·kg^{-1} (≈3–8 ppm), the capacity of C-S-H phases for the uptake of strongly sorbing metal ions (*e.g.* Ln(III), An(III, IV, VI), Be(II)) has been reported as 0.1 mol·kg^{-1} and beyond [41,79,80]. Based on this comparison, we speculate on the preferential retention of ^{95}Nb/^{93}Nb by C-S-H phases, even though acknowledging that the capacity of C-S-H phases for the uptake of Nb(V) has not been characterized yet.

The very high distribution coefficients determined in this work for the uptake of Nb(V) by HCP are in line with data reported for other strongly sorbing metal ions, *e.g.* Th(IV) (log R_d ≈ 5–7) [41], Sn(IV) (log R_d ≈ 4–5.5) [9] or Be(II) (log R_d ≈ 5–6) [80,90]. In spite of the evident chemical differences between these elements, all of them are characterized by a high charge-to-size ratio, $z/d > 1$, where z is the charge of the metal ion and d is the M-O interatomic distance (d $r_M^{z+} + r_O^{2-}$): z/d[Nb^{5+}] 2.36, z/d[Th^{4+}] 1.61, z/d[Sn^{4+}] 1.82, z/d[Be^{2+}] 1.20 [39]. The ratio z/d was previously considered by Wieland and Van Loon [8] to qualitatively describe the sorption trends observed for different metal ions, although the authors acknowledged that this approach implicitly emphasizes the ionic character of the bonding independently of the underlying uptake mechanism. Similar correlations are commonly used to explain trends in the hydrolysis of metal ions (see for instance [81]), thus reflecting the close relationship between hydrolysis and sorption in the case of strongly hydrolyzing metal ions.

There are virtually no data for the uptake of vanadium or tantalum (both belonging to group V of the periodic table, as Nb) by cement. The comparison of the sorption properties of Nb(V) with other pentavalent elements is not evident, and has not been attempted previously in the literature. Within a comprehensive study dedicated to the uptake of neptunium (+IV, +V and +VI) by cementitious systems, Tits and co-workers reported a very strong sorption of Np(V) on C-S-H phases (log R_d ≈ 6) [82]. Pentavalent neptunium is characterized by the formation of the very stable linear "-yl" moiety, *i.e.* $[O{=}Np{=}O]^+$, which in hyperalkaline conditions (with pH ≥ 12) is predominantly found as $NpO_2(OH)_2^-$ or $NpO_2(OH)_3^{2-}$ [83,84]. Although these species show clear structural and steric differences with respect to $Nb(OH)_7^{2-}$, we note that the aqueous speciation of Nb(V) in hyperalkaline systems is not well stablished, and the predominance of species like $NbO_2(OH)_4^{3-}$ as previously proposed by [58] may approach the chemistry of Nb(V) in hyperalkaline systems to that of An(V) or An(VI). Note that in hyperalkaline systems containing calcium, Fellhauer and co-workers reported also the formation of ternary complexes Ca(II)-Np(V)-OH [85,86] and analogous species might be also expected for Nb(V).

4.4. Uptake of Nb(V) by HCP in the presence of ISA

The impact of ISA on the uptake of Nb(V) by cement was investigated using two different order of addition of the individual components: (i) (^{95}*Nb* + *cement*) + *ISA*, and (ii) (^{95}*Nb* + *ISA*) + *cement*. In both cases, the third component was added to the system after a pre-equilibration time of 2 days. Sequence (i) can accordingly be interpreted as a desorption experiment in the presence of ISA. Sorption data determined for both systems are shown in Fig. 6 as log R_d *vs.* log $[ISA]_{aq}$, where $[ISA]_{aq}$ corresponds to the concentration of ISA in solution, which was calculated on the basis of the initial ISA concentration and the ISA sorption isotherm described in [52]. Dashed line in the figure corresponds to the calculated stability limit of HCP expressed in terms of % CaO present in HCP (right scale). The decrease in the % CaO is calculated based on the inventory of CaO in HCP, the S/L in the experiment (1 g·L^{-1}) and the dissolved Ca concentration due to the formation of Ca-ISA complexes. For the highest $[ISA]_{aq}$, this calculation shows that ≈50% of the original CaO has been dissolved from HCP, thus indicating that the uptake of Nb(V) at this ISA concentration is possibly underestimated due to the loss of HCP material. The figure includes also experimental data for the uptake of Th(IV) by HCP (degradation stage I) in the presence of ISA as reported by [87].

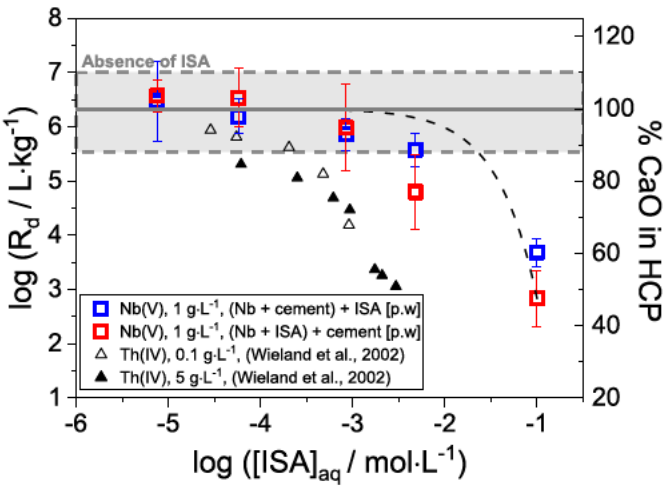

Fig. 6. Values of log R_d (with R_d expressed in L·kg^{-1}) determined in this work for the uptake of ^{95}Nb(V) by HCP degradation phase I in the presence of ISA. All experiments conducted for S:L = 1 g·L^{-1}. Only active niobium (^{95}Nb) used in the experiments. The different symbols reflect the order of addition of the individual components: blue squares: (Nb + cement) + ISA; red squares: (Nb + ISA) + cement. Black symbols correspond to the uptake of Th(IV) by HCP in the degradation stage I under increasing ISA concentrations as reported by Wieland and co-workers [87]. The concentration of ISA in solution $[ISA]_{aq}$ was calculated on the basis of the initial ISA concentration and the ISA sorption isotherm described in [52]. The term [p.w.] stands for present work. (For interpretation of the references to color in this figure legend, the reader is referred to the web version of this article.)

Fig. 6 shows a clear decrease in the sorption of Nb(V) at log $[ISA]_{aq}$ above ≈ 3. This observation is attributed to the formation of stable Nb(V)-ISA complexes in the aqueous phase. As discussed in Section 2, similar complexes as those reported for Zr(IV) ($Zr(OH)_4(ISA)_2^{2-}$ and $Zr(OH)_4(ISA)(ISA_{-H})^{3-}$) [34] can be expected for the Nb(V)-ISA system. Note that at pH 13.5, the complexes Zr(IV)-ISA become predominant above log $[ISA]_{aq}$ ≈ 4.2, in line with the range of ISA concentration for which an impact on the uptake of Nb(V) by cement is observed.

The decrease in log R_d values observed in Fig. 6 is more accentuated (*ca.* 0.5 log-units) for the sequence (^{95}Nb + *ISA*) + *cement*. Similar observations were reported by Tasi and co-workers for the system cement-Pu-ISA [33]. Long-term experiments conducted by the latter authors (with $t \leq 490$ days) showed that the uptake for the sequence (*Pu* + *ISA*) + *cement* is kinetically hindered, and that equilibrium conditions are attained faster for the sequence (*Pu* + *cement*) + *ISA*. Due to the limitations imposed by the use of short-lived isotopes of Nb, the conclusions derived in [33] from their long-term experiments are also adopted in the present work with regard to the order of addition for the system cement-Nb-ISA. Thus, it is expected that equilibrium has been obtained in the (^{95}Nb + *cement*) + *ISA* system whilst this is not the case in (^{95}Nb + *ISA*) + *cement*.

Fig. 6 shows a weaker impact of ISA on the uptake of Nb(V) by cement (this work) compared to the Th(IV) system [87], in both cases using a HCP in the degradation stage I. Data reported by Wieland et al. for Th(IV) are taken as a representative example to assess the impact of ISA on the retention of a strongly sorbing metal ion by cement. The evolution of sorption data (R_d values) with increasing ISA concentration shown in Fig. 6 reflects the formation of weaker aqueous complexes for the system Nb(V)-ISA than for Th(IV)-ISA. Wieland and co-workers explained the decrease in the log R_d values with increasing ISA concentration by the formation of stable ternary complexes Ca-Th(IV)-ISA in the aqueous phase. Such ternary complexes have been also described for the system Ca-Pu(IV)-ISA [29], and should probably be expected for the ternary system Ca-Nb(V)-ISA.

4.5. Uptake of Nb(V) by cement in the presence of Cl^- and Cl^- + ISA

The impact of chloride on the uptake of Nb(V) by cement was investigated with a series of sorption experiments in the absence and in the presence of ISA, with $[ISA]_{aq}$ 0.1 M as calculated from $[ISA]_0$ and using the ISA sorption isotherm described in [52]. All experiments were performed using only active niobium, with $[^{95}Nb]$ $4.5 \cdot 10^{-12}$ and $1.8 \cdot 10^{-12}$ M for experiments conducted in the absence and in the presence of ISA, respectively. Initial chloride concentrations were corrected for the chloride leached by cement ($[Cl^-]_{leached}$ $1.1 \cdot 10^{-4}$ M, for S:L 1 $g \cdot L^{-1}$), as experimentally determined in this work. Fig. 7 shows the Nb(V) uptake in the presence of 10^{-3} M ≤ $[Cl^-]_0$ ≤ 0.1 M (absence of ISA) and $1.1 \cdot 10^{-4}$ M ≤ $[Cl^-]_0$ ≤ 1.0 M (presence of ISA). The figure includes also sorption data for the niobium uptake by NRVB in saline water conditions, *i.e.* 0.5 M NaCl, as reported by [23].

No significant impact of Cl^- on the sorption of Nb(V) was observed in the absence of ISA. Hence, log R_d values determined for the ternary system cement-Nb(V)-Cl^- are slightly lower but in agreement with those obtained in the corresponding chloride-free systems (green region in Fig. 7). Slightly lower log R_d values were reported by Baker and co-workers for the uptake of Nb(V) by NRVB in the presence of 0.5 M NaCl [23]. The difference in the distribution coefficients determined in this work and reported by Baker et al. can be possibly explained on the basis of the different cementitious materials used in both studies, *i.e.* CEM I (this work) and NRVB [23], as well as differences in the experimental conditions, *e.g.* pH (13.5 *vs.* 12.2), S:L (0.1 $g \cdot L^{-1}$ *vs.* 20 $g \cdot L^{-1}$) or phase separation methods.

C-S-H phases have been reported to remain stable up to 1 M NaCl, as interpreted by the constant Si concentration measured in pore water solutions containing up to this salt concentration [24,88]. However, ion exchange processes in the C-S-H phases do occur, resulting in the partial substitution of Ca by Na and the consequent increase of Ca concentration

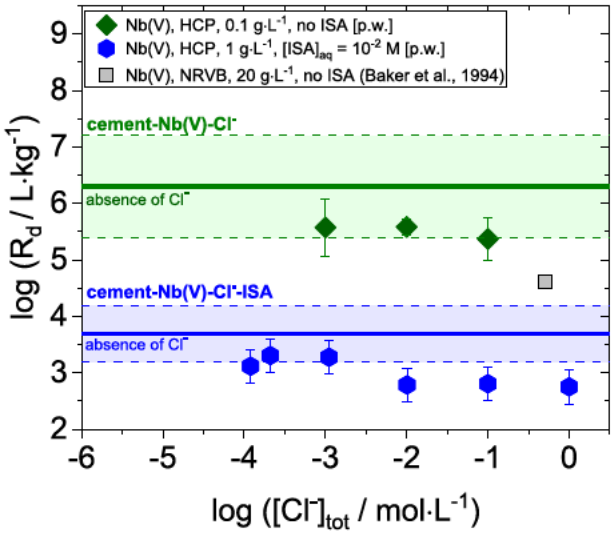

Fig. 7. Distribution coefficients determined in this work for the uptake of $^{95}Nb(V)$ by HCP (deg. stage I) in the presence of chloride (green symbols, 10^{-3} M ≤ $[Cl^-]_0$ ≤ 0.1 M, S:L = 0.1 $g \cdot L^{-1}$), and in the presence of chloride and ISA (blue symbols, $1.1 \cdot 10^{-4}$ M ≤ $[Cl^-]_0$ ≤ 1.0 M, $[ISA]_{aq}$ = 0.1 M, S:L = 1 $g \cdot L^{-1}$). Total concentrations of chloride in solution, $[Cl^-]_{tot}$, account also for the chloride content leached from cement, as determined experimentally in this work. Solid and dashed lines indicate average log R_d values and corresponding uncertainties in the absence of chloride and ISA (green lines) and in the absence of chloride and presence of ISA (blue lines). Grey symbol shows the uptake of Nb(V) by NRVB in the presence of 0.5 M NaCl, as reported by Baker et al. [23]. The term [p.w.] stands for present work. (For interpretation of the references to color in this figure legend, the reader is referred to the web version of this article.)

in the pore water [24,88]. This effect leads also to an overall decrease of the Ca:Si ratio in the C-S-H phases or cement exposed to saline conditions. Fig. 5 in Section 4.3 shows also a very strong uptake of Nb(V) (log R_d ≈ 5–5.5) by C-S-H phases and HCP with Ca:Si ratios lower than that considered in the present study. This observation provides additional support to the strong uptake of Nb(V) in cement systems containing high concentrations of NaCl, even if the composition of the C-S-H phases is impacted at high chloride concentrations as discussed in the literature.

Sorption data determined for the quaternary system cement -Nb(V)-Cl^--ISA with $[ISA]_{aq}$ 0.1 M and $[Cl^-]_{tot} \leq 10^{-3}$ M are in moderate agreement with log R_d values obtained for chloride-free systems containing the same ISA concentration (blue region in Fig. 7). A slight decrease in the overall sorption is observed at higher chloride concentrations, although log R_d values and corresponding uncertainties almost overlap with the distribution coefficients determined for chloride-free systems. The competition of ISA with the sorption of other anionic radionuclides has been previously reported in the literature. Hence, Pointeau and co-workers observed a slight decrease in the uptake of SeO_3^{2-} by HCP at [ISA] ≥ 10^{-3} M [89], and hypothesized that this might be caused by the competition between both negative species for the sorption sites available on the surface of the HCP. Although the effect observed in the present work is relatively small, high concentrations of chloride in solution (*i.e.* ≥10^{-2} M) may have a similar impact on the uptake of ISA. This hypothesis remains to be confirmed by additional experimental evidence, *e.g.* with systematic sorption experiments with ISA under increasing chloride concentrations.

5. Conclusions

A comprehensive series of sorption experiments were conducted under Ar atmosphere to assess the uptake of niobium by cement in the

degradation stage I (fresh hydrated cement). Experiments aimed also at evaluating the impact of ISA and chloride on the uptake of Nb, given the relevance of both components in specific waste streams in L/ILW. Due to the very low niobium concentrations imposed by the formation of sparingly soluble Ca-Nb(V) oxide phases in cement pore water ($\approx 10^{-8}$–10^{-6} M), sorption experiments were conducted using the short-lived isotope ^{95}Nb ($t_{1/2}$ 31.15 days) generated by the irradiation of a natural Zr target in the cyclotron at the research facility HZDR Leipzig. Experiments were conducted under the variation of key parameters, *i.e.* $1 \cdot 10^{-15}$ M $\leq [Nb]_{tot} \leq 1 \cdot 10^{-9}$ M (with $[Nb]_{tot}$ $[^{95}Nb] + [^{91m}Nb] + [^{93}Nb]$), 0.1 g·L^{-1} $\leq$ S:L $\leq$ 10 g·L^{-1}, $t \leq$ 54 days, $1 \cdot 10^{-5}$ M $\leq [ISA]_{tot} \leq$ 0.1 M and $1.1 \cdot 10^{-4}$ M $\leq [Cl^-]_{tot} \leq$ 1.0 M.

The concentrations of niobium in pristine HCP and in YCWCa equilibrated with HCP were quantified as (3.1 ± 0.3) ppm (*i.e.* (3.3 ± 0.3) • 10^{-5} mol·kg^{-1}) and (8 ± 3) • 10^{-10} M, respectively. Oversaturation solubility experiments conducted in the YCWCa revealed that a pyrochlore-structure Ca-Nb(V) oxide is responsible for the solubility control of Nb(V), defining niobium concentrations at equilibrium of $[Nb(V)]_{aq}$ $7 \cdot 10^{-8}$–$2 \cdot 10^{-6}$ M. This value is considered as upper concentration limit of niobium in the pore water of the investigated cement systems, and served as input parameter in the definition of the sorption experiments.

A fast ($t \approx 2$ days) and very strong uptake of niobium ($5 \leq \log R_d \leq 7$) was observed for all experiments conducted in the absence of ISA. These values are consistent with previous sorption studies with ^{95}Nb conducted in the presence of C-S-H phases or cement in the degradation stages II and III. Severe discrepancies identified with other studies reporting much weaker sorption ($\log R_d \approx$ 1–4) are attributed to the only use of inactive niobium (^{93}Nb) in the latter studies. Some of these results are biased by the high initial concentrations of ^{93}Nb and the corresponding solubility-control of the system, whereas the correct interpretation of those studies using low initial ^{93}Nb concentrations requires the consideration of the ^{93}Nb content in pristine HCP. Isotopic exchange with ^{93}Nb present in HCP is considered as plausible retention mechanism for ^{95}Nb, although the uptake by calcium silicate hydrate (C-S-H) phases is tentatively proposed as main retention process on the basis of the high affinity of these phases for the uptake of Nb(V) and their large inventory in HCP. In analogy with previous studies conducted with hard Lewis acids forming negatively charged hydrolysis species in cement pore water, we hypothesize that Ca^{2+} ions play a key role in bridging the negatively charged Nb(V) hydrolysis species to the C-S-H surface.

Experiments performed in the presence of ISA were interpreted accounting for the sorption of this ligand on the cement material investigated in the present work (see [52]). ISA was found to importantly decrease the uptake of Nb(V) at $[ISA]_{aq} \geq 10^{-3}$ M, with $\log R_d \approx 3.5$ being quantified at $\log [ISA]_{aq} \approx$ 1. This observation is attributed to the formation of stable (Ca-)Nb(V)-ISA complexes in the aqueous phase, as previously described in the literature for the systems Zr(IV)-ISA, An(III)/Ln(III)-ISA or An(IV)-ISA. The order of addition of the individual components was found to have an impact on the overall sorption, with the sequence (*Nb* + *cement*) + *ISA* resulting in enhanced R_d values (*i.e.* stronger sorption). By analogy with experiments performed for the system cement-Pu(IV)-ISA, we conclude that the uptake observed for the sequence (*Nb* + *ISA*) + *cement* is kinetically hindered and thus does not represent equilibrium conditions. Although high chloride concentrations are known to affect the structure of C-S-H phases, the uptake of niobium in the absence and presence of ISA remained mostly unaltered within the range of chloride concentrations investigated in this study.

This work provides a comprehensive quantitative description of the uptake of niobium by cementitious materials, which so far was lacking for the degradation stage I of cement. This new information allows the correct quantification of the retention of niobium in the context of the Safety Case for underground or near-surface repositories for nuclear waste. It provides also a thorough scientific basis for the future development of more detailed thermodynamic/geochemical models, *e.g.* in the form of aqueous-solid solution models.

Declaration of competing interest

The authors declare that they have no known competing financial interests or personal relationships that could have appeared to influence the work reported in this paper.

Acknowledgements

This work was partly funded by ONDRAF-NIRAS. KIT-INE acknowledges HZDR for support in providing the irradiated Zr foil used to prepare the ^{95}Nb stock solution. Frank Geyer, Annika Kaufmann and Melanie Bottle (all KIT–INE) are gratefully acknowledged for the ICP–MS/OES measurements and technical support. Thanks are due to Dieter Schild and Agost Tasi (both KIT–INE) for SEM analyses and fruitful discussions on the cement-RN-ISA system, respectively. Luc Van Loon and Martin Glaus (PSI-LES) are kindly acknowledged for providing the α-isosaccharino-1,4-lactone used in this study. Yukio Tachi (JAEA) is gratefully acknowledged for fruitful discussions on the cement-Nb system.

Appendix A. Supplementary data

Supplementary data to this article can be found online at https://doi.org/10.1016/j.cemconres.2021.106690.

References

[1] J.P. Collier, H.W. Song, J.C. Phillips, J.K. Tien, The effect of varying Al, Ti, and Nb content on the phase-stability of Inconel-718, metallurgical transactions a-physical metallurgy and materials, Science 19 (1988) 1657–1666.
[2] L. Wang, E. Martens, D. Jacques, P.D. Canniere, J. Berry, D. Mallants, Review of sorption values for the cementitious near field of a near surface radioactive waste disposal facility, in: Project Near Surface Disposal of Category A Waste at Dessel, ONDRAF/NIRAS Technical Report, NIROND-TR Report 2008-23E, NIRAS-MP5-03 DATA-LT(NF), Version 1, Brussels, Belgium, 2009.
[3] J.P. Adams, M.L. Carboneau, National Low-Level Waste Management Program Radionuclide Report Series, Volume: 11 Niobium-94, DOE/LLW-127, Idaho National Engineering Laboratory, Idaho, United States of America, 1995.
[4] G.Z. He, S. Jiang, Z.Y. Zhou, M. He, W.Z. Tian, J.L. Zhang, L.J. Diao, H. Li, Precise half-life measurement for the ground state of nb-94, Phys. Rev. C 86 (2012).
[5] R.P. Schuman, P. Goris, Half-life and decay of Niobium-94, J. Inorg. Nucl. Chem. 12 (1959) 1–5.
[6] A.G. Espartero, J.A. Suarez, M. Rodriguez, Determination of nb-93m and nb-94m in medium and low level radioactive wastes, Appl. Radiat. Isot. 49 (1998) 1277–1282.
[7] ONDRAF/NIRAS, Hoofdstuk 14 - Veiligheidsevaluatie - Langetermijnveiligheid - Veiligheidsrapport voor de oppervlaktebergingsinrichting van categorie A-afval te Dessel, in: Category A. Technical Report NIROND-TR 2011-14 V3, Brussels, Belgium, 2019.
[8] E. Wieland, L.Van Loon, Cementitious Near-Field Sorption Data Base for Performance Assessment of an ILW Repository in Opalinus Clay. Technical Report 3-06, Paul Scherrer Institut, Villigen, Switzerland, 2003.
[9] M. Ochs, D. Mallants, L. Wang, Radionuclide and Metal Sorption on Cement and Concrete, Springer, Switzerland, 2016.
[10] U.R. Berner, Evolution of porewater chemistry during degrardation of cement in a radioactive waste repository environment, Waste Manag. 12 (1992) 201–219.
[11] A. Atkinson, N. Everitt, R. Guppy, Evolution of pH in a rad-waste repository: Internal reactions between concrete constituents, in: UKAEA Report, AERE-R12939, Harwell, UK, 1988.
[12] S. Gaboreau, S. Grangeon, F. Claret, D. Ihiawakrim, O. Ersen, V. Montouillout, N. Maubec, C. Roosz, P. Henocq, C. Carteret, Hydration properties and interlayer Organization in Synthetic C-S-H, Langmuir 36 (2020) 9449–9464.
[13] B. Lothenbach, A. Nonat, Calcium silicate hydrates: solid and liquid phase composition, Cem. Concr. Res. 78 (2015) 57–70.
[14] C.F. Baes, R.E. Mesmer, The Hydrolysis of Cations, John Wiley & Sons, New York, 1976.
[15] P.L. Brown, C. Ekberg, Hydrolysis of Metal Ions, Wiley-VCH Cerlag GmbH, Weinheim, 2016.
[16] A.J. Bard, R. Parsons, J. Jordan, Standard Potentials in Aqueous Solution, Marcel Dekker Inc., New York, 1985.
[17] C. Peiffert, C. Nguyen-Trung, D.A. Palmer, J.P. Laval, E. Giffaut, Solubility of B-Nb2O5 and the hydrolysis of Niobium(V) in aqueous solution as a function of temperature and ionic strength, J. Solut. Chem. 39 (2010) 197–218.
[18] G.J.P. Deblonde, A. Chagnes, S. Belair, G. Cote, Solubility of niobium(V) and tantalum(V) under mild alkaline conditions, Hydrometallurgy 156 (2015) 99–106.
[19] B. Lothenbach, M. Ochs, D. Hager, Confinement of radioactive waste in cementitious barriers for surface and deep geological disposal, in: ANDRA Report, CRP OBMG, 1999, 99-001.

[20] I. Pointeau, C. Landesman, N. Coreau, N. Moisan, P. Reiller, Etude de la retention chimique des radionucleides Cs(I), Am(III), Zr(IV), Pu(IV), Nb(V), U(VI), Tc(IV) par les matériaux cimentaires degradés, in: CEA/DEN/SAC Report RT DPC/SECR 03-037, 2004.
[21] C. Talerico, M. Ochs, E. Giffaut, Solubility of niobium(V) under cementitious conditions: importance of ca-niobate, Mater. Res. Soc. Symp. Proc. 842 (2004) 443–448.
[22] J.J. Pilkington, N.S. Stone, The solubility and sorption of nickel and niobium under high pH conditions, NSS/R186 (1990) 1–46.
[23] S. Baker, R. McCrohon, P. Oliver, N.J. Pilkington, The sorption of niobium, tin, iodine and chlorine onto nirex reference vault backfill, Mater. Res. Soc. Symp. Proc. 333 (1994) 719–724.
[24] E. Wieland, Sorption Data Base for the Cementitious Near Field of L/ILW and ILW Repositories for Provisional Safety Analyses for SGT-E2, Nagra Technical Report 14-08, Paul Scherrer Institut, Villigen, Switzerland, 2014.
[25] M.A. Glaus, L.R. van Loon, S. Achatz, A. Chodura, K. Fischer, Degradation of cellulosic materials under the alkaline conditions of a cementitious repository for low and intermediate level radioactive waste part I: identification of degradation products, Anal. Chim. Acta 398 (1999) 111–122.
[26] M.A. Glaus, L.R. Van Loon, Degradation of cellulose under alkaline conditions: new insights from a 12 years degradation study, Environ. Sci. Technol. 42 (2008) 2906–2911.
[27] K. Vercammen, M.A. Glaus, L.R. Van Loon, Complexation of Th(IV) and Eu(III) by alpha-isosaccharinic acid under alkaline conditions, Radiochim. Acta 89 (2001) 393–401.
[28] J. Tits, E. Wieland, M.H. Bradbury, The effect of isosaccharinic acid and gluconic acid on the retention of Eu(III), Am(III) and Th(IV) by calcite, Appl. Geochem. 20 (2005) 2082–2096.
[29] A. Tasi, X. Gaona, D. Fellhauer, M. Bottle, J. Rothe, K. Dardenne, R. Polly, M. Grive, E. Colas, J. Bruno, K. Kallstrom, M. Altmaier, H. Geckeis, Thermodynamic description of the plutonium - alpha-D-isosaccharinic acid system ii: formation of quaternary Ca(II)-Pu(IV)-OH-ISA complexes, Appl. Geochem. 98 (2018) 351–366.
[30] D. Rai, N.J. Hess, Y.X. Xia, L.F. Rao, H.M. Cho, R.C. Moore, L.R. Van Loon, Comprehensive thermodynamic model applicable to highly acidic to basic conditions for isosaccharinate reactions with Ca(II) and Np(IV), J. Solut. Chem. 32 (2003) 665–689.
[31] W. Hummel, G. Anderegg, L. Rao, I. Puigdomenech, O. Tochiyama, Chemical Thermodynamics of Compounds and Complexes of U, Np, Pu, Am, Tc, Se, Ni and Zr With Selected Organic Ligands, Elsevier, North-Holland, Amsterdam, 2005.
[32] X. Gaona, V. Montoya, E. Colas, M. Grive, L. Duro, Review of the complexation of tetravalent actinides by ISA and gluconate under alkaline to hyperalkaline conditions, J. Contam. Hydrol. 102 (2008) 217–227.
[33] A. Tasi, X. Gaona, T. Rabung, D. Fellhauer, J. Rothe, K. Dardenne, J. Lutzenkirchen, M. Grive, E. Colas, J. Bruno, K. Kallstrom, M. Altmaier, H. Geckeis, Plutonium retention in the isosaccharinate - cement system, Applied Geochemistry 126 (2021).
[34] T. Kobayashi, T. Teshima, T. Sasaki, A. Kitamura, Thermodynamic model for zr solubility in the presence of gluconic acid and isosaccharinic acid, J. Nucl. Sci. Technol. 54 (2017) 233–241.
[35] A.D. Moreton, N.J. Pilkington, C.J. Tweed, Thermodynamic Modeling of the Effect of Hydrocarboxylic Acids on the Solubility of Plutonium at High pH, Nuclear Industry Radioactive Waste Executive (Nirex), UK, 2000.
[36] M.R. Gonzalez-Siso, X. Gaona, L. Duro, M. Altmaier, J. Bruno, Thermodynamic model of Ni(II) solubility, hydrolysis and complex formation with ISA, Radiochim. Acta 106 (2018) 31–45.
[37] F. Fairbrother, D. Robinson, J.B. Taylor, Water-soluble complexes of niobium (Columbium) and tantalum. 2. The dissolution of niobic and tantalic acids in amine solutions, J. Chem. Soc. (1958) 2074–2079.
[38] F. Fairbrother, J.B. Taylor, Water-soluble complexes of niobium (Columbium) and tantalum. 1. Complexes with alpha-hydroxy-acids and (2-Hydroxyethyl)Amines, J. Chem. Soc. (1956) 4946–4954.
[39] R.D. Shannon, Revised effective ionic radii and systematic studies of interatomic dsitances in halides and chalcogenides, Acta CrystA 32 (1976) 751–767.
[40] J. Bruno, M.R. González-Siso, L. Duro, X. Gaona, M. Altmaier, Key master variables affecting the mobility of Ni, Pu, Tc and U in the near field of the SFR repository, in: Main Experimental Findings and PA Implications of the PhD Thesis, SKB Tehcnical Report, 18-01, Svensk Karnbranslehantering AB, Solna, Sweden, 2018.
[41] J. Tits, E. Wieland, Actinide sorption by cementitious materials, in: PSI Technical Report, 18-02, Paul Schwerer Institute, Villigen, Switzerland, 2018.
[42] B.F. Greenfield, H. M.H., M.W. Spindler, H.P. Thomason, The Effect of the Products from Anaerobic Degradation of Cellulose on the Solubility and Sorption of Radioelements in the Near Field, Nuclear Industry Radioactive Waste Executive (Nirex), UK, 1997.
[43] A. Geochem, Actinide chemistry source term, DOE/WIPP-19-3609, in: Title 40 CFRPart 191 Subparts B and C Compliance Recertification Applications 2019, United States Department of Energy, WIPP, United States, 2019.
[44] J.F. Lucchini, B. M., H. Khaing, M.K. Richman, J.S. Swanson, K. Simmons, D. T. Reed, WIPP Actinide-Relevant Brine Chemistry, LCO-ACP-15, LANL/ACRSP Report. LAUR 13-20620, Los Alamos National Laboratory, New Mexico, United States, 2013.
[45] W. Brewitz, F + E Programm zur Eignungsprüfung der Schachtanlage Konrad für die Einlagerung radioaktiver Abfalle - Zusammenfassender Zwischenbericht, GSF-T 114, Braunschweig, 1981.
[46] S.K. Frape, P. Fritz, R.H. Mcnutt, Water rock interaction and chemistry of groundwaters from the Canadian shield, Geochim. Cosmochim. Acta 48 (1984) 1617–1627.
[47] S. Nagasaki, T. Saito, T.T. Yang, Sorption behavior of Np(V) on illite, shale and MX-80 in high ionic strength solutions, J. Radioanal. Nucl. Chem. 308 (2016) 143–153.
[48] L. Duro, V. Montoya, E. Colàs, D. García, Groundwater Equilibration and Radionuclide Solubility Calculations, Nuclear Waste Management Organization, TR-2010-02, Ontario, Canada, 2014.
[49] H. Allan, Long-term Safety for KBS-3 Repositories at Forsmark and Laxemar -A First Evaluation Main Report of the SR-Can Project, SKB-TR-06-09, Swedish Nuclear Fuel and Waste Management Company, Stockholm, Sweden, 2006.
[50] L. Duro, M. Grivé, E. Cera, X. Gaona, C. Domènech, J. Bruno, E.S. S.L., Determination and Assessment of the Concentration Limits to be Used in SR-Can, SKB-TR-06-32, Swedish Nuclear Fuel and Waste Management Co, Stockholm, Sweden, 2006.
[51] C. Peiffert, C. Nguyen-Trung, P. Landais, Etude experimentale de la solubilite des oxydes de Nb(V) cristallise et amorphe dans des solutions aqueuses, in: ANDRA Report, C RP 0CRE 97-003, 1997.
[52] Y. Jo I. Androniuk N. Cevirim-Papaioannou B.D. Blochouse M. Altmaier X. Gaona , Uptake of Chloride and Iso-saccharinic Acid by Cement: Sorption and Molecular Dynamics Studies on HCP (CEM I) and CSH, (Under Review at Cement and Concrete Research).
[53] Y. Jo, N. Çevirim-Papaioannou, X. Gaona, K. Garbev, B. Blochouse, M. Altmaier, Solubility of niobium(V) in hyperalkaline systems containing ca: characterization of the solubility-controlling solid phases in cementitious environments, in: 19th International Symposium on Solubility Phenomena and Related Equilibrium Processes (ISSP19), 2021.
[54] E. Giffaut, M. Grive, P. Blanc, P. Vieillard, E. Colas, H. Gailhanou, S. Gaboreau, N. Marty, B. Made, L. Duro, Andra thermodynamic database for performance assessment: ThermoChimie, Appl. Geochem. 49 (2014) 225–236.
[55] D.D. Wagman, W.H. Evans, V.B. Parker, R.H. Schumm, I. Halow, S.M. Bailey, K. L. Churney, R.L. Nuttall, The NBS tables of chemical thermodynamic properties - selected values for inorganic and C-1 and C-2 organic-substances in si units, J. Phys. Chem. Ref. Data 11 (1982) 1–392.
[56] T.B. Lindemer, T.M. Besmann, C.E. Johnson, Thermodynamic review and calculations - alkali-metal oxide systems with nuclear-fuels, fission-products, and structural-materials, J. Nucl. Mater. 100 (1981) 178–226.
[57] M. Altmaier, V. Neck, T. Fanghanel, Solubility of Zr(IV), Th(IV) and Pu(IV) hydrous oxides in CaCl(2) solutions and the formation of ternary ca-M(IV)-OH complexes, Radiochim. Acta 96 (2008) 541–550.
[58] A. Goiffon, R. Granger, C. Bockel, B. Spinner, Investigation of equilibria in niobium-V alkaline solutions, Rev. Chim. Mineral. 10 (1973) 487–502.
[59] K. Vercammen, Complexation of Calcium, Thorium and Europium by a Isosaccharic Acid Under Alkaline Conditions Dissertation No 134666, ETH, Zürich, 2000.
[60] R.L. Whistler, B. J.N., A-D-isosaccharino-1,4-lactone, action of lime water on lactose, in: M.L. Wolfrom, J.N. BeMiller (Eds.), Methods in Carbohydrate Chemistry, Vol. 2: Reactions of Carbohydrates 477-449, Academic Press, New York, United States of America, 1963.
[61] S. Busse, J. Brockmann, F. Rosch, Radiochemical separation of no-carrier-added radioniobium from zirconium targets for application of nb-90-labelled compounds, Radiochim. Acta 90 (2002) 411–415.
[62] V. Radchenko, D.V. Filosofov, O.K. Bochko, N.A. Lebedev, A.V. Rakhimov, H. Hauser, M. Eisenhut, N.V. Aksenov, G.A. Bozhikov, B. Ponsard, F. Roesch, Separation of nb-90 from zirconium target for application in immuno-PET, Radiochim. Acta 102 (2014) 433–442.
[63] J.S. Erskine, M.L. Sink, L.P. Varga, Solvent extraction separation of tantalum and niobium florides with n-benzoyl-n-phenylhydroxylamine, Analytical Chemistry 41 (1969), 70-&.
[64] M. Filella, P.M. May, The aqueous solution thermodynamics of niobium under conditions of environmental and biological interest, Appl. Geochem. 122 (2020).
[65] O.L. Keller, Identification of complex ions of Niobium(V) in hydrofluoric acid solutions by Raman and infrared spectroscopy, Inorg. Chem. 2 (1963) 783.
[66] J.E. Land, C.V. Osborne, Formation constants of niobium fluoride system, J. Less Common Met. 29 (1972) 147.
[67] W.G. Faix, R. Caletka, V. Krivan, Element distribution coefficients for hydrofluoric- acid nitric acid-solutions and the anion-exchange resin dowex 1x8, Anal. Chem. 53 (1981) 1719–1721.
[68] E.P. Horwitz, R. Chiarizia, M.L. Dietz, H. Diamond, Separation and preconcentration of actinides from acidic media by extraction chromatography, Anal. Chim. Acta 281 (1993) 361–372.
[69] E.P. Horwitz, M.L. Dietz, R. Chiarizia, H. Diamond, A.M. Essling, D. Graczyk, Separation and preconcentration of uranium from acidic media by extraction chromatography, Anal. Chim. Acta 266 (1992) 25–37.
[70] G.M. Marinov, A.P. Marinova, D.V. Medvedev, J.A. Dadakhanov, M.M. Milanova, S. Happel, V.I. Radchenko, D.V. Filosofov, Determination of distribution coefficients (K-d) of various radionuclides on UTEVA resin, Radiochim. Acta 104 (2016) 735–742.
[71] C. Cachoir, P.D. Canniere, F. Druyts, K. Ferrand, B. Kursten, K. Lemmens, T. Mennecart, E. Valcke, in: Preparation of Evolved Cement Water (ECW) and Young Cement Waters (YCW and YCWCa) for the Supercontainer experiments, IW. W&D.0088, 2006, pp. 1–9.
[72] B. Lothenbach, F. Winnefeld, Thermodynamic modelling of the hydration of Portland cement, Cem. Concr. Res. 36 (2006) 209–226.
[73] JCPDS, Powder diffraction files, in: Joint Committee on Powder Diffraction Standards, Swarthmore, USA, 2001.
[74] H.F.W. Taylor, Cement Chemistry, second ed., Thomas Telford, London, 1997.
[75] E. Wieland, J. Tits, P. Spieler, J.P. Dobler, Interaction of Eu(III) and Th(IV) with sulfate-resisting Portland cement, MRS Proc. 506 (1997) 573.

[76] J. Tits, T. Stumpf, T. Rabung, E. Wieland, T. Fanghanel, Uptake of Cm(III) and Eu (III) by calcium silicate hydrates: a solution chemistry and time-resolved laser fluorescence spectroscopy study, Environ. Sci. Technol. 37 (2003) 3568–3573.
[77] Y. Tachi, T. Suyama, M. Mihara, Data Acquisition for Radionuclide Sorption on Barrier Materials for Performance Assesement f Geological Disposal of TRU Wastes, JAEA-Data/Code 2019-021, Japan Atomic Agency, 2-4 Shirakata, Tokai-mura, Naka-gun, Ibaraki-ken, 319-1195 Japan, 2020.
[78] E. Wieland, J. Tits, A. Ulrich, M.H. Bradbury, Experimental evidence for solubility limitation of the aqueous Ni(II) concentration and isotopic exchange of Ni-63 in cementitious systems, Radiochim. Acta 94 (2006) 29–36.
[79] J. Tits, T. Stumpf, E. Wieland, T. Fanghanel, The immobilisation of Eu(III) and Cm (III) by calcium silicate hydrates, Geochim. Cosmochim. Acta 67 (2003) A482.
[80] N. Çevirim-Papaioannou, I. Androniuk, S. Han, N. Ait Mouheb, S. Gaboreau, W. Um, X. Gaona, M. Altmaier, Sorption of beryllium in cementitious systems relevant for nuclear waste disposal: quantitative description and mechanistic understanding (accepted), Chemosphere 282 (2021) 131094, https://doi.org/10.1016/j.chemosphere.2021.131094.
[81] V. Neck, J.I. Kim, Solubility and hydrolysis of tetravalent actinides, Radiochim. Acta 89 (2001) 1–16.
[82] J. Tits, X. Gaona, A. Laube, E. Wieland, Influence of the redox state on the neptunium sorption under alkaline conditions: batch sorption studies on titanium dioxide and calcium silicate hydrates, Radiochim. Acta 102 (2014) 385–400.
[83] D. Fellhauer, X. Gaona, K. Dardenne, M. Altmaier, Solubility and speciation of neptunium(V) in alkaline, dilute to concentrated NaCl, MgCl2 and CaCl2 solutions, in: 17th International Symposium on Solubility Phenomena and Related Equilibrium Processes (ISSP17), July 24-29 Geneva, Switzerland, 2016.
[84] V.G. Petrov, D. Fellhauer, X. Gaona, K. Dardenne, J. Rothe, S.N. Kalmykov, M. Altmaier, Solubility and hydrolysis of Np(V) in dilute to concentrated alkaline NaCl solutions: formation of na-Np(V)-OH solid phases at 22 °C, Radiochim. Acta 105 (2017) 1–20.
[85] D. Fellhauer, M. Altmaier, X. Gaona, J. Lutzenkirchen, T. Fanghanel, Np(V) solubility, speciation and solid phase formation in alkaline CaCl2 solutions. Part I: experimental results, Radiochimica Acta 104 (2016) 355–379.
[86] D. Fellhauer, M. Altmaier, X. Gaona, J. Lutzenkirchen, T. Fanghanel, Np(V) solubility, speciation and solid phase formation in alkaline CaCl2 solutions. Part II: Thermodynamics and implications for source term estimations of nuclear waste disposal, Radiochimica Acta 104 (2016) 381–397.
[87] E. Wieland, J. Tits, J.P. Dobler, P. Spieler, The effect of alpha-isosaccharinic acid on the stability of and Th(IV) uptake by hardened cement paste, Radiochim. Acta 90 (2002) 683–688.
[88] J. Hill, A.W. Harris, M. Manning, A. Chambers, S.W. Swanton, The effect of sodium chloride on the dissolution of calcium silicate hydrate gels, Waste Manag. 26 (2006) 758–768.
[89] I. Pointeau, N. Coreau, P.E. Reiller, Uptake of anionic radionuclides onto degraded cement pastes and competing effect of organic ligands, Radiochim. Acta 96 (2008) 367–374.
[90] N. Çevirim-Papaioannou, S. Han, I. Androniuk, W. Um, M. Altmaier, X. Gaona, Uptake of Be(II) by Cement in Degradation Stage I: Wet-Chemistry and Molecular Dynamics Studies, Minerals 11 (10) (2021) 1149, https://doi.org/10.3390/min11101149.